



بسم الله الرحمن الرحيم



Sudan University of Science & Technology

College of Graduate Studies

Geometrically Non-linear Finite Element Analysis of Plane Stress Structures Using MATLAB Programme

التحليل الهندسي اللاخطي بالعنصر المحدد لمنشآت الاجهاد المستوي
بإستخدام برنامج الماتلاب

*A Thesis submitted to Department of Structural Engineering College of
Engineering in partial fulfillment of the requirements of the degree of Master
of Science in Civil Engineering (Structures)*

Prepared by:

Abdullatif Yousif Mohammed Adam

(B.Sc (Hon), Nyala University, 2011)

Supervisor:

Prof/Abd Elrahman Elzubeir Mohamed

March 2017

بِسْمِ اللَّهِ الرَّحْمَنِ الرَّحِيمِ

(وَإِذْ يَرْفَعُ إِبْرَاهِيمُ الْقَوَاعِدَ مِنَ الْبَيْتِ وَإِسْمَاعِيلُ رَبَّنَا تَقَبَّلْ
مِنَّا ۖ إِنَّكَ أَنْتَ السَّمِيعُ الْعَلِيمُ (127))

صدق الله العظيم ...

(سورة البقرة)

Dedication

To the meaning of love and compassion ...

To the mystery of existence and the meaning of life ...

To my Mather

My sisters....

I dedicate this work

ACKNOWLEDGEMENT

First all praise and thanks are to Allah, who helped me to complete this work.

I would like to express sincere appreciation and gratitude to my Supervisor *professor. Dr. A/Elrahman Elzubeir Mohamed*, for his teaching, guidance, patience, and above all as supervisor.

I also want to thanks and my gratitude to teachers, colleagues, friend, and all who contributed to the completion of this research.

My infinite gratitude to my small family, my mother, my sisters

Finally, I would like to thank *Nyala University foundation*.

Abstract

In this research Total Lagrangian formulation for geometric nonlinear plane stress problems was developed. The formulation is based on Green strains and 2nd Piola-Kirchoff stresses. The formulation was applied on two- dimensional elasticity using 4-node plane finite element. The formulation was implemented as a finite element program using MATLAB (2010b). The program was developed for linear and nonlinear analysis of plane stress structure subjected to different types of loading.

The solution of nonlinear equilibrium equation was obtained by incremental method with Newton-Raphson approach. The program was applied to obtain nodal displacements, direct stresses and shear stresses at integration points of element based on Green strains and 2nd Piola-Kirchoff stresses.

The accuracy of results was demonstrated by using three numerical examples for linear analysis. The results were in very good agreement when compared with results from references and known exact solutions. It was, also observed from Graphs and Tables that the results show high accuracy with mesh refinement and increment applied load.

For the nonlinear analysis, the resulting displacements show good agreement when compared with known results or published papers results.

تجريد

في هذا البحث تم تطوير الصيغ الهندسية اللاخطية لمنشآت اجهاد المستوي الواحد باستخدام تقنين لاجرانج الكلي (Total Lagrangian) بناء على انفعالات قرين واجهادات بيولا كريتشوف الثانية, هذه الصيغ طبقت علي المرونة ثنائية الابعاد باستخدام عنصر الاربع عقد المحدد.

تم تطبيق الصيغ بتطوير برنامج عنصر محدد باستخدام لغة البرمجة ماتلاب (2010b). طور البرنامج للتحليل الخطي واللاخطي لمنشآت الاجهاد المُستوي المعرضة لانواع مختلفة من الاحمال.

حل معادلات الاتزان اللاخطية بني علي طريقة الاحمال التزايدية و طريقة نيوتن - رابسون . طبق البرنامج للحصول علي الازاحات عند العقد والاجهادات المباشرة واجهادات القص عند نقاط التكامل (integration point) بناء علي انفعالات قرين واجهادات بيولا كريتشوف الثانية .

وقد نلاحظ, ايضاً, من الجداول والمخططات, ان هنالك تزايد في دقة النتائج مع زيادة عدد العناصر وازدياد الاحمال المطبقة.

تم التحقق من دقة النتائج بأستخدام ثلاثة امثلة عددية, التحليل الخطي اعطت النتائج المتحصل عليها توافقاً جيداً جداً مقارنة بالحلول الدقيقة المعروفة والمنشورة. اما في حالة التحليل اللاخطي فقد اعطت النتائج توافقاً جيداً مع النتائج المنشورة في عدة اوراق علمية.

Contents	page
A. Verse	I
B. Dedication	II
C. Acknowledgements	III
D. Abstract in Arabic	IV
E. Abstract	V
F. Table of contents	VI
G. List of tables	VII
H. List of figures	VIII
I. List of symbols	IX

Chapter one: General introduction

1.1 General introduction	1
1.2 Problems statement	3
1.3 Objective of research	4
1.4 Methodology	5
1.5 Outline of thesis	5

Chapter two: Literature review

2.1 Introduction to finite element analysis method	6
2.2 Using MATLAB finite element programming	7
2.3 Sources of nonlinearity in finite element analysis	8
2.3.1 Geometric nonlinearities	8
2.3.2 Material nonlinearities	8
2.3.3 Force nonlinearities	8
2.3.4 Kinematic nonlinearities	8
2.4 Total Lagrangian and Updated Lagrangian formulation	9
2.4.1 Comparison of T.L and U.L formulation	9

2.5 Stress – Strain Measures	9
2.6 Brief description of the finite element method	11
2.7 Previous studies	12
2.8 Non-linear solution techniques	14
2.8.1 Introduction	14
2.8.2 Newton -Raphson method	14
2.8.3 Modified Newton- Raphson method	15
2.8.4 Incremental Force Method	15
Chapter three: Geometrically non-linear finite element of plain stress/ strain	
3.1 Introduction	17
3.2 Finite Element formulation of 4-node Isoperimetric plane stress/strain element	18
3.2.1 Introduction	18
3.2.2 Stress-strain relation	19
3.2.3 Incremental formulations for geometrically nonlinear plane stress/ strain Element	22
3.3 Theory method of formulation for plane stress/strain element	25
3.3.1 Stress-strain relation	25
3.3.2 Strain-displacement relation	25
3.3.3 Green's Lagrangian strain	26
3.3.4 Stiffness matrix due to Green strain	26
3.4 Incremental equilibrium equations	30
Chapter four: Implementation and Application program and Verification	
4.1 Computer program for linear and non-linear finite element for plane stress/strain using MATLAB	32

4.1.1	Introduction	32
4.1.2	Main program procedures	32
4.1.3	Program layout	34
4.1.4	Function explanations	36
4.2	Verification of formulation	37
4.2.1	Introduction	37
4.2.2	Linear analysis	37
4.2.2.1	Cantilever plate beam under concentrated load at the end	37
4.2.2.2	Cantilever plate beam under pure bending	44
4.2.2.3	Simple supported plate beam under udl	50
4.2.3	Nonlinear analysis	55
4.2.3.1	Clamped plate beam under concentrated load	55
4.2.3.2	Cantilever plate beam under pure bending	57
4.2.3.3	Discussion of result	59
Chapter five: Conclusions and Recommendations		
5.1	Summary of work	62
5.2	Conclusions	62
5.3	Recommendations	63
References		64
Appendix A		66
Appendix B		72

List of Tables

Table	Description	page
Table (4.1)	Vertical displacement at free end and mesh effect	42
Table (4.2)	Vertical displacement at the free end	43
Table (4.3)	Vertical displacement at point A (200EL, 5INC)	44
Table (4.4)	Vertical displacement at point A (200EL, 10INC)	44
Table (4.5)	Vertical displacement at point A (200EL, 15INC)	44
Table (4.6)	Deflected shape along center line (100EL)	45
Table (4.7)	Stress in x-direction at integration point (INT1)	46
Table (4.8)	Stress in y-direction at integration point (INT1)	46
Table (4.9)	Shear stress at integration point (INT1)	47
Table (4.10)	Vertical Displacement at free end and with aspect ratio	49
Table (4.11)	Vertical Displacement at free end	49
Table (4.12)	Vertical displacement at free end (200EL, 4INC)	50
Table (4.13)	Vertical displacement at free end (200EL, 8INC)	50
Table (4.14)	Vertical displacement at free end (200EL, 12INC)	51
Table (4.15)	Deflected shape along center line (60EL)	51
Table (4.16)	Stress in x-direction at integration point (EL (1), INT 1)	52
Table (4.17)	Stress in y-direction at integration point (EL (1), INT 1)	53
Table (4.18)	Shear stress at integration point (EL (1), INT 1)	53
Table (4.19)	Vertical displacement at mid-span	55
Table (4.20)	Vertical displacement at mid-span different element	55
Table (4.21)	Deflected shape along center line (220EL)	56
Table (4.22)	Stress in x-direction at integration point at mid-span (INT 1)	57

Table (4.23) Shear Stress at integration point at mid-span (INT 1)	58
Table (4.24) Vertical displacement at mid-span (Clamped)	59
Table (4.25) Deflected shape along center line (Clamped)	60
Table (4.26) Vertical displacement at free end (pure bending)	62
Table (4.27) Deflected shape along center line (pure bending)	62

List of Figures

Figures	Description	Page
Fig (2.1)	Configuration change during deformation	9
Fig (2.2)	Newton-Raphson Method	14
Fig (2.3)	Modified Newton-Raphson Method	15
Fig (2.4)	Incremental Force method	16
Fig (3.1)	Total Lagrangian	17
Fig (3.2)	Updated Lagrangian	17
Fig (3.3)	4-node Isoperimetric element	18
Fig (3.4)	4-node Gauss Points	19
Fig (3.5)	Deformed and Undeformed Shape	26
Fig (4.1)	Main program flow chart	36
Fig (4.1a)	Flow chart of NONA2D function	38
Fig (4.1b)	Flow chart of LINA2D function	39
Fig (4.2)	Cantilever plate beam with vertical load at free end	42
Fig (4.3)	Effect of mesh and aspect ratio on accuracy of results	43
Fig (4.4)	Vertical displacement at point A	43
Fig (4.5)	Deformed shape along center line	45
Fig (4.6)	Stress in x-direction at integration point (El 1)	46
Fig (4.7)	Stress in y-direction at integration point (El 1)	47
Fig (4.8)	Shear stress at integration point (El 1)	47
Fig (4.9)	Cantilever plate under pure bending	48
Fig (4.10)	Effect of mesh and aspect ratio on accuracy of results	49
Fig (4.11)	Vertical displacement at free end at point A	50
Fig (4.12)	Deformed shape along center line	52

Fig (4.13) Stress in x-direction at integration point (INT 1, El 1)	52
Fig (4.14) Stress in y-direction at integration point (INT 1, El 1)	53
Fig (4.15) Shear stress at integration point (INT 1, El 1)	54
Fig (4.16) Simple supported plate beam under uniform load	54
Fig (4.17) Vertical displacement at mid -span	55
Fig (4.18) Deformed shape along center line	57
Fig (4.19) Stress at integration point in x-direction at El (108,118)	57
Fig (4.20) Shear stress at integration point at El (108,118)	58
Fig (4.21) Clamped plate beam under concentrated load (Non-linear)	59
Fig (4.22) Vertical displacement at mid-span (Non-linear)	60
Fig (4.23) Deformed shape along center line (Non-linear)	61
Fig (4.24) Cantilever plate under pure bending (Non-linear)	61
Fig (4.25) Vertical displacement at free end point A (Non-linear)	62
Fig (4.26) Deformed shape along center line	63

List of Symbols

Symbol	Description
FEA	Finite element analysis
σ_E	Engineering stress
A_0	Original area
σ_c	Cauchy stresses (true)
L_0	Original length
$[k]_e$	Element stiffness matrix
$[\delta]_e$	Element nodal displacement vector
$[F]_e$	Element Nodal force vector
ε	Green strain
D	Elastic matrix
J	Jacobian matrix
r, s	Natural coordinates
ε_0	Linear strain vector
ε_L	Nonlinear strain
A	Matrix containing displacement derivative
θ	Vector containing displacement derivative
a	Vector of nodal displacement
B_0	Linear strain-displacement transformation matrix

B_L	Nonlinear strain-displacement transformation matrix
$F_{11}, F_{12}, F_{21}, F_{22}$	Component of deformation gradient vector
g_x, g_y	Displacement gradient vector
φ	Residual force
G	Nonlinear strain-displacement transformation matrix
K_0	Displacement stiffness matrix
K_L	Large displacement stiffness matrix
M	Initial stress matrix
K_σ	A symmetrical initial stress stiffness matrix
K_T	Total tangential stiffness matrix
ΔU	Incremental displacement
El	Element
INT	Integration point
INC	Increment
Udl	uniform distribution load

Chapter one

General introduction

1.1 Introduction

The finite element method is a numerical technique for solution of differential equations. In this method all complexities of the problems like varying shape, boundary conditions and loads are maintained as they are, but the solutions obtained are approximate.

The finite element method originated as a method of stress analysis in the design of aircraft .It started as an extension of matrix method of structure analysis. Nowadays this method is used not only for the analysis of solid mechanics, but even in the analysis of fluid flow, heat transfer, electric and many other physical phenomena. In civil engineering is used this method extensively for the analysis of beams, space frames, plates, shells, foundations, Both static and dynamic problems can be handled by finite element method (Bhavikatti,2005).

Finite element method is a powerful technique for obtaining approximate solution with good accuracy. The particular advantages of finite element method have made it the most accepted design tool and the greatest advantage of it is ability to handle truly arbitrary geometry. Probably its other most important features are the ability to deal with general boundary conditions and to include non-homogeneous and anisotropic materials, nonlinear stress- strain relations, nonlinear strain-displacement relations and complicated loading conditions (Akasha, 2009).

Nonlinear finite element analysis is an essential component of computer-aided design. Testing of prototypes is increasingly being replaced by simulation

with nonlinear finite element methods because this provides a more rapid and less expensive way to evaluate design concepts and design detail.

Both analysts and developers of nonlinear finite element programs should understand the fundamental concepts of nonlinear finite element analysis. Without an understanding of the fundamentals, a finite element program is a black box that provides simulations. However, nonlinear finite element analysis confronts the analyst with many choices and pitfalls. Without an understanding of the implication and meaning of these choices and difficulties, an analyst is at a severe disadvantage (Belytschison, et. el, 2013).

Two sources of nonlinearity exist in the analysis of solid continua, namely, material and geometric nonlinearity. The former occurs when, for whatever reason, the stress strain behavior given by the constitutive relation is nonlinear, whereas the latter is important when changes in geometry, whether large or small, have a significant effect on the load deformation behavior. the geometric nonlinearity includes deformation-dependent boundary conditions and loading.

The nonlinear strain and stress measures in definition of stress-strain relation are one of key concepts of several nonlinearities. Strain is defined as change of the shape or geometry produced by applied load. The loads are defined by the general term stress (Kim, 2014).

To practically assess the stress state on the structure, strain must be measured. There are alternative strain measures used to derive finite element equations, such as Green's strain which is associated with 2nd Piola-Kirchhoff stress, engineering strain which is associated with engineering stress and logarithmic strain which is associated with true (Cauchy) stress. The Green's strain is most common definition applied to materials used in mechanical and structural engineering problems, which are subjected to small deformations. The engineering strain is expressed as the ratio of total deformation to initial dimension of the material body in which the loads are being applied. The logarithmic strain also called natural strain or true strain is based on the final

deformed dimension and considering an incremental strain and obtained by integrating this incremental strain (Akasha and Mohamed, 2012).

The fast improvements in computer hardware technology and slashing of cost of computers have boosted this method, since the computer is the basic need for its application of this method. A number of popular brand of finite element analysis packages are now available commercially. Some of the popular packages are STAAD-PRO, GT-STRUDEL, NASTRAN and ANSYS. Using these packages one can analyze several complex structures.

MATLAB is commercial software and a trademark of The Math Works, Inc., It is an integrated programming system, and MATLAB is getting increasingly popular all fields of science and engineering.

MATLAB presently offers a nice combination of handy programming features with powerful built-in numerical capabilities. On the one hand, its m-file programming environment allows researchers to implement moderately complicated algorithms in a structured and coherent fashion. On the other hand, its built-in, numerical capabilities empower researchers to solve more difficult problems.

MATLAB is a high-level language specially designed for dealing with matrices. This makes it particularly suited for programming the finite element method. In addition, MATLAB will allow the user to focus on the finite element method by alleviating the programming burden (Khennan, 2013).

1.2 Problem statement

For many structures, the relation between the deflection and the applied load is linear when the deflection is small. This includes small strain, small displacement, and small rotation. But in case of the large deflection the relation becomes nonlinear.

If the structure system is solved using the linearity assumption, the results may end up physically inexact, because the linear analysis uses the undeformed geometry which lead to invalid result. Also many engineering applications cannot be modeled as linear system when the deformation is large.

For above reasons the study focuses to using geometrically nonlinear analysis.

The available commercial packages are only used as a closed box. That is, given data in a certain format to give results in a well organized manner. Also, difficulty in obtaining original copies of these commercial packages leads to the need for developing finite element programs that are original and that can be easily modified. This helps in having an efficient research tool (Khennan, 2013).

Minimizing the overall cost of analysis and obtaining a good result of analysis reduce risk of resulting design errors.

Since MATLAB is getting increasingly popular computer software in all fields of engineering, especially in finite element analysis and design of structure, it was used in this research.

1.3 Objectives

The objectives of the study are:

- 1- To use the MATLAB for programming of the plane stress/strain problems using geometrically nonlinear finite element analysis.
- 2- To formulate the geometric nonlinear Total Lagrangian elasticity problems using plane stress/ strain isoparametric finite element based on Green's strain.
- 3- To develop a computer program based on the formulation.
- 4- To implement the program on computer using MATLAB language.
- 5- To verify and check the accuracy of the results obtained from application of the program by comparison with known published results.

1.4 Methodology of Research

The methodology of research as the following:

- 1- Finite element formulation using 4-node plane stress/ strain element.
- 2- The formulation based on Green strain was considered. Linear and geometrically nonlinear analysis based on Green strain was adopted. The nonlinear equilibrium equations solved using the incremental with Newton-Raphson method.

3- The main computer program in MATLAB language was developed and the formulation was implemented in it. The program was designed to carry out linear analysis and geometric nonlinear analysis based on Green stress, for linear elastic isotropic material.

4- The program was applied and tested using numerical examples to obtain the displacement, direct stresses and shear stresses at integration points of the element. The results obtained were discussed, analyzed, and compared with known results.

1.5 Outlines of research

This study covers three main areas, the introduction of finite element method (FEM) and the literature review, geometrically nonlinear formulation of plane stress/strain, implementation of the formulation into MATLAB program. The contents can be summarized as:

Chapter one: Contains general introduction of finite element method, problem, statement, objectives, methodology and outline of dissertation.

Chapter two: presents the literature review

Chapter three: contains the general description of nonlinear method and development of the formulation of geometric nonlinear plane strain/stress finite element.

Chapter four: contains the description of the computer program

Chapter five: presents the results and discussion of results, conclusions and recommendations for further work.

Chapter two

Literature review

2.1 Introduction to Finite Element Analysis Method

The finite element method is one of the numerical methods for solving differential equations that describe many engineering problems. The finite element method (FEM), originated in the area of structural mechanics, has been extended to other areas of solid mechanics and later to other fields such as heat transfer, fluid dynamics, and electromagnetism. In fact, FEM has been recognized as a powerful tool for solving partial differential equations and integrodifferential equations, it has become the numerical method of choice in almost all engineering and applied science areas. One of the reasons for FEM's popularity is that the method results in computer programs versatile in nature that can solve many practical problems with least amount of training (Kim, 2014).

In modern engineering design it is rare to find a project that does not require some type of finite element analysis. The greatest advantage of FEM is its ability to handle truly arbitrary geometry. Probably its next most important features are the ability to deal with general boundary conditions and to include non-homogeneous and anisotropic materials. These features mean that systems of arbitrary shape that are made up of numerous different material regions. Each material could have constant properties or the properties could vary with spatial location. To these very desirable features a large amount of freedom in prescribing the loading conditions and in the post processing of items such as the stresses and strains etc.

The classes of problems include stress analysis, heat conduction, electrical fields, magnetic fields, ideal fluid flow (Akin, 2000).

In comparison with classical methods, it's clearly seen that:

1. In classical methods exact equations are formed and exact solutions are obtained where as in finite element analysis exact equations are formed but approximate solutions are obtained.
2. Solution have been obtained for few standard cases by classical method, where as solutions can be obtained for all problems by FEM.
3. FEM can handle structures with anisotropic properties without any difficulty, in classical methods when material property is not isotropic, solution for problems become very difficulty.
4. If the structure consists of more than one material, it is difficult to use classical methods, but FEM can be used without any difficult.
5. Problems with material and geometric nonlinearities cannot be handle by classical methods. (Bhavikatti, 2005).

2.2 Using MATLAB in Finite Element Programming

Understanding basic program structure of finite element analysis is important for better comprehension of the FEM. MATLAB is especially convenient to write and understand FEM programs because a MATLAB program manipulates matrices and vectors with ease. MATLAB is interactive software which has been used in various areas of engineering and scientific applications, It is not a computer language in the normal sense but it does most of the work of a computer language, One attractive aspect of MATLAB is that it is relatively easy to learn, and it does not require in-depth knowledge on operational principles of computer programming like compiling and linking in most of other programming languages.

The power of MATLAB is represented by the length and simplicity of the code; Numerical calculation in MATLAB uses collections of well written scientific/mathematical subroutines as LINPACK and EIPACK. MATLAB Provides Graphical user interface (GUI) as well as three dimensional graphical animations (Young, 1997).

2.3 Sources of Nonlinearity in Structures

1- Geometric Nonlinearities

Geometric nonlinearities represent the cases when the relations among displacement quantities, whether translations and/or rotation are nonlinear. They can also occur when rotations are large, even with small deformation (Kim, 2014).

2- Material Nonlinearities

Material nonlinearity represents the case when the relation between stress and strain is not linear. This relation is often referred to as the constitutive relation. In the linear system the elastic modulus matrix $[D]$ is constant, when the stress-strain relation cannot be represented by a constant matrix, $[D]$.

3- Force Nonlinearities

Force nonlinearity occurs when the applied forces depend on deformations. Since force is a vector, its magnitude or direction can change according to the deformation of a structure. Force nonlinearity is often accompanied by geometric nonlinearity.

4- Kinematic Nonlinearity

Kinematic nonlinearity is also called boundary nonlinearity, as the displacement boundary conditions depend on the deformation of the structure. When the boundary conditions change as a function of displacements, both the displacements and boundary conditions are unknown.

2.4 Total Lagrangian and Updated Lagrangian Formulations

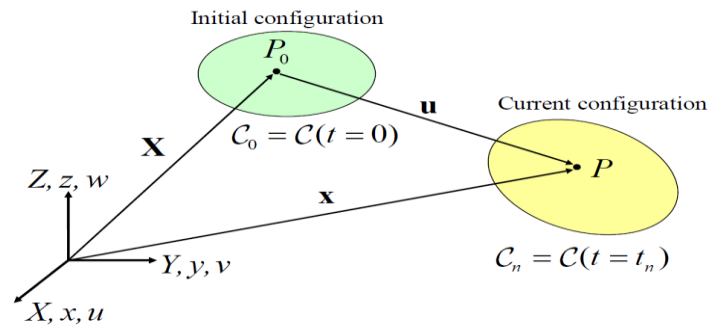


Fig (2.1) Configuration change during deformation

In The total Lagrangian formulation (T.L.) refers all the static and kinematic variables to the initial configuration. The updated Lagrangian (U.L.) formulation is based on the same process as in the T.L. formulation, but it's refers all static and kinematic variables to the last in equilibrium configuration

❖ Comparison of T.L and U.L formulations is listed as follows:

- 1- In the T.L formulation, all derivatives are with respect to initial coordinates where as in U.L formulation, all derivatives are with respect to the current coordinates.
- 2- In the U.L formulation the calculated updated stresses represent the actual physical stresses (true stresses)
- 3- The same assumptions are made in the linearization and indeed almost the same finite element stiffness and force vectors are calculated
- 4- The linear strain displacement matrix is complicated in the total Lagrangian formulation than the Updated Lagrangian formulation because the effect of the term involving the initial displacement.

2.5 Stress and Strain Measures

The description of deformation and the measure of strain are essential parts of nonlinear finite element continuum mechanics. In general structural

components or continuum bodies will exhibit large strain when undergoing a geometrically nonlinear deformation process.

The main Stress measures are (Bathe et. al., 1975):

1- Engineering stress

Defined in terms of the original area and the original geometry

2- Cauchy (true) stress

Define in terms of current area and current deformed geometry.

3- 1st Piola-Kirchhoff stress

Defined in terms of the original area and the current deformed
Geometry

4- 2nd Piola- Kirchhoff stress

Defined in terms of the initial area and current deformed geometry for small strain, the 2nd Piola-Kirchhoff stress can be interpreted as the true stress related to local axes that rotate with the material.

The corresponding Strain measures are:

1- Engineering strain

$$e_E = (L - L_0)/L_0 \quad (2.1)$$

A measure preferred by structural engineers, and work conjugate to the engineering stress measure.

2- Logarithmic (natural)strain

$$e_L = \ln\left(\frac{L}{L_0}\right) \quad (2.2)$$

A measure that is incremental in form and work conjugate to the Cauchy stress measure.

This measure is typically used for large strain analysis.

3- Green Lagrange strain

$$e_G = (L^2 - L_0^2)/2L_0 \quad (2.3)$$

It is work conjugate to the 2nd Piola-Kirchhoff stress measure.

2.6 Brief description of the finite element method

In solid mechanics the unknown field variable is displacement. In a continuum, these unknowns are infinite. The finite element procedure reduces such unknowns to a finite number by dividing the solution region into small parts called elements and by expressing the unknown field variables in terms of assumed approximating shape functions within each element. The approximating functions are defined in terms of field variables of specified nodal points. Once these are found the field variables at any point can be found by using the interpolating shape functions.

After selecting elements nodal unknowns, the next steps in finite element analysis is to determine element properties for each element. The element stiffness matrix and load vector are given mathematically, by the relationship:

$$[K]_e \{\delta\}_e = \{F\}_e \quad (2.4)$$

Where

$[K]_e$ is the element stiffness matrix

$\{\delta\}_e$ Is element nodal displacement vector and $\{F\}_e$ is element nodal force vector

The element of stiffness matrix k_{ij} represents the force in coordinate direction, I, due to a unit displacement in coordinate direction j. Four methods are available for formulating these element properties. direct approach, variation approach, weighted residual approach and energy balance approach. Any one of these methods can be used for assembling element properties. In solid mechanics variation approach is commonly employed to assemble stiffness matrix and nodal force vector (Bhavikatti, 2005).

Element properties are used to assemble global properties/ structural properties to get system equation;

$$[K]\{\delta\} = \{F\} \quad (2.5)$$

Where

$[K]$ Is the global stiffness matrix

$\{\delta\}$ Is global nodal displacement vector and $\{F\}$ is global nodal force vector

Then the boundary conditions are imposed. And the solution of these simultaneous equations gives the nodal unknowns. Using these nodal values additional calculations are made to get the required gradients e.g. stresses and strains.

Thus, the steps involved in the finite element analysis are:

1. Select suitable field variables and the elements.
2. Discretize the continua
3. Select interpolation functions.
4. Find the element properties.
5. Assemble element properties to get global properties.
6. Impose the boundary conditions.
7. Solve the system of equations to get the nodal unknowns.
8. Make additional calculations to get the required values.

2.7 Previous Studies

There are many applications of plane stress/strain element in different fields of analysis.

Pida, Yang and Soedel, 1989 used large strain 8-node plane stress Isoparametric finite element for prediction of rubber fraction. The formulation is based on total Lagrangian and incremental formulation.

Mohamed, 1983 used both Green strain and engineering strain measures to solve thin beam problems. He also, proposed total Lagrangian modified incremental equations for a two-dimensional state of stress based on the engineering strains.

Cook, 1995 stated that geometric nonlinearity (as opposed to material nonlinearity) arises when deformations are large enough to significantly affect applied load. The goal of analysis is to construct the nonlinear relation between applied load and the resulting deformation. He assumed that the surfaces are sufficiently thin that large displacements are possible without yielding of the material.

Zienkiewicz, 2000 introduced the geometric nonlinear analysis using the Lagrangian formulation, with incremental procedure combined with Newton-Raphson iterative techniques.

Mohammed, 2009 performed the geometric nonlinear analysis of isoparametric Quadrilateral Elements and the formulation of 4-noded quadrilateral isoparametric element. He also developed finite element analysis code to model the geometric nonlinear solid element, and verified of the code by some examples and comparison with analytical solution

Mohamed and Adam, 2003 presented a finite element formulation for large deformation analysis of shells; the three-dimension 8-noded isoparametric finite element was adopted. A Total Lagrangian formulation by using Engineering strain and Green strain were used in derivation of the geometric element stiffness matrix. The nonlinear equilibrium equations were solved by combined incremental load and Newton-Raphson method.

Mellierr, 1969 presented a thesis on a finite element analysis for geometrically nonlinear large displacement problems in thin elastic plates and shells. In his study only stable equilibrium configuration was considered Engineering strains were assumed to remain small, the geometrical stiffness of the resulting eighteen degree of freedom triangular element was derived from a purely geometrical stand point. The geometrical stiffness was linked with the standard small displacement stiffness and was used in the linear incremental approach to obtain numerical solution to the large displacement problems.

Akasha and Mohamed, 2012 developed a formulation for geometric nonlinear plane stress/strain based on logarithmic strain. That formulation was coupled with modifying a formulation based on a engineering strain. A geometric nonlinear Total Lagrangian formulation was adopted for two – dimensional elasticity using 4-node plane finite elements. The solution of nonlinear equation was obtained by Newton-Raphson method.

AbdElazeez, 2015 developed a formulation for geometric nonlinear finite element of cantilever beam based on Green strain. The formulation was

implemented on computer by using MATLAB program. The incremental method was used in solving nonlinear equilibrium equations.

2.8 Nonlinear solution techniques

2.8.1 Introduction

The finite element formulation for nonlinear problems requires to solution techniques to solve the system of nonlinear equations. The solution procedure may even influence the formulation of the problem.

Different methods are available according to the way to calculate the displacement increment, as follows:

2.9.2 Newton-Raphson Method

This method is popular in numerical analysis to find the roots of nonlinear equations. Basically, most numerical methods for solving a system of nonlinear equations assume an initial estimate, \mathbf{u}^0 and find its increment, $\Delta\mathbf{u}$ so that new estimate, $\mathbf{u}^0 + \Delta\mathbf{u}$, is close to the solution to equation (3.33). In order to find the increment, the nonlinear equations are locally approximated by linear once. This process is repeated until the original nonlinear equations are satisfied as shown in Fig (2.2).

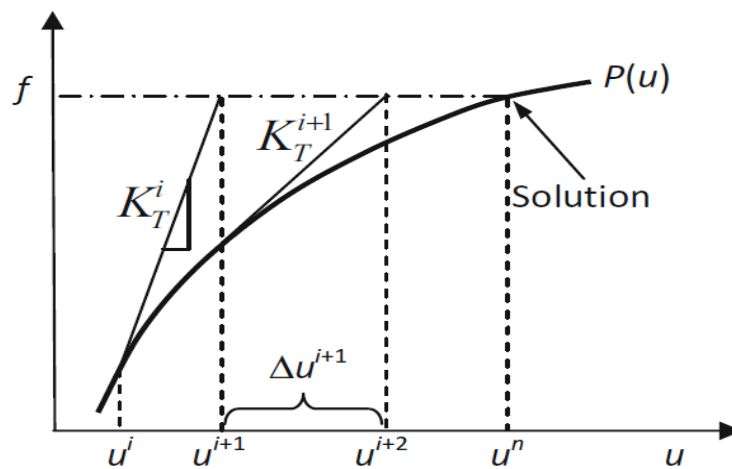


Fig (2.2) Newton-Raphson method

2.9.3 Modified Newton-Raphson Method

At the iteration process the Newton-Raphson Method requires forming the Jacobian matrix and the system of linearized equations should be solved for each increment of solution. Computationally, these are expensive tasks. In the finite element framework, building the tangent stiffness matrix and solving the matrix equation are the two most computationally intensive procedures. The modified Newton-Raphson method is an attempt to make these procedures less expensive. Instead of formulating a new tangent stiffness matrix at each iteration, the initial tangent stiffness matrix is repeatedly used in all iterations as shown in Fig (2.3).

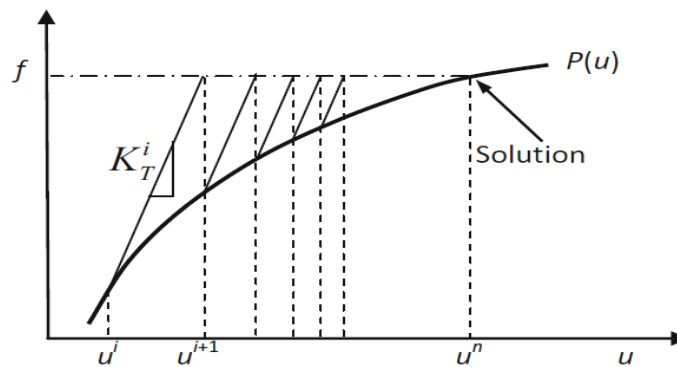


Fig (2.3) Modified Newton-Raphson method

2.9.4 Incremental Force Method

The idea of the incremental force method is to apply the load in increments. Within each load increment, the procedure is the same as the standard Newton-Raphson method. The next load increment is applied after the solution corresponding to the current load increment has converged. The converged solution at each increment is then used as an initial estimate of the next increment as shown in Fig (2.4).

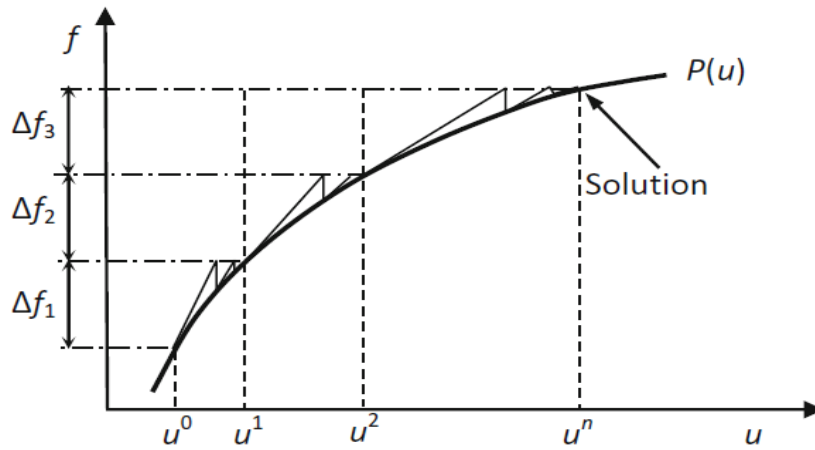


Fig (2.4) Incremental force method

The following chapter presents the finite element formulation of 4- node element and theory of geometrically nonlinear plane stress/strain problems.

Chapter Three

Geometrically Non-linear Finite Element Analysis of Plane Stress/Strain Problems

3.1 Introduction

Geometric nonlinearity arises when change in geometry whether large or small, has a significant effect on the load deformation behavior. Geometric nonlinearity includes deformation-dependent boundary conditions and loading.

As a direct consequence of geometric nonlinearity, the stiffness matrix of the finite element model is not constant. It is a function of the residual displacement. Therefore, an iterative procedure is required to obtain the equilibrium state.

For a given load, there are two main Lagrangian formulations depending on the configuration to which the variables involved in each step are referred. These are:

1. The Total Lagrangian formulation where all variables are referred to initial configuration in Fig (3.1).



Fig (3.1) Total Lagrangian

2. The Updated Lagrangian formulation where all the variables are referred to the configuration at the beginning of the load step considered in Fig (3.2).

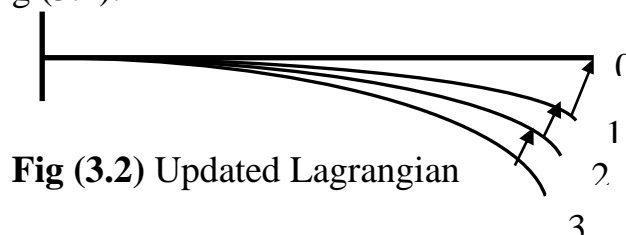


Fig (3.2) Updated Lagrangian

3.2 Formulations of The 4-node Isoparametric Plane Stress/ Strain Element:

3.2.1 Introduction

The bilinear quadratic element as shown in Fig (3.3) and Fig (4.3) is a two dimensional finite element with both local and global coordinates. It is characterized by linear shape functions in each of the x and y directions. This element can be used for plane stress or plain strain problems in elasticity. It is a generalization of the 4-node rectangular element (Pattan, 2008).

A Total Lagrangian formulation based on 4-node isoparametric plane stress/strain using Green's strain with 2nd Piola-Kirchhoff is adopted in this chapter.

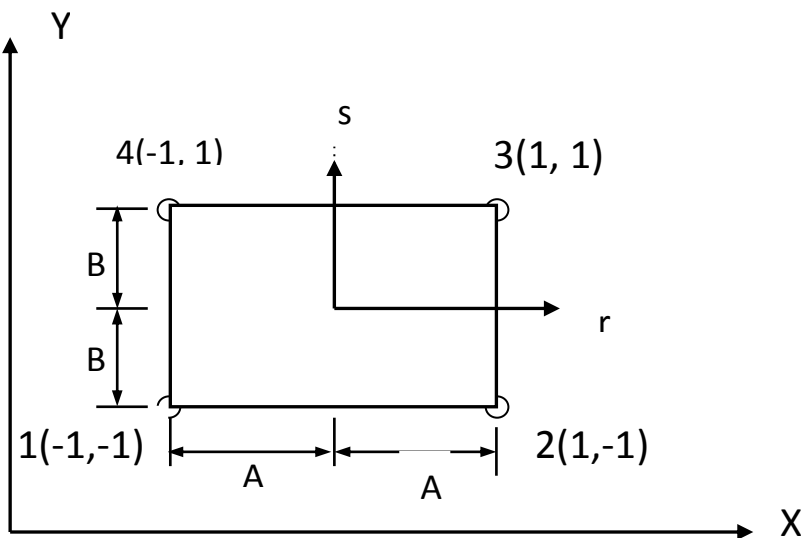


Fig (3.3) 4-node Isoparametric Element

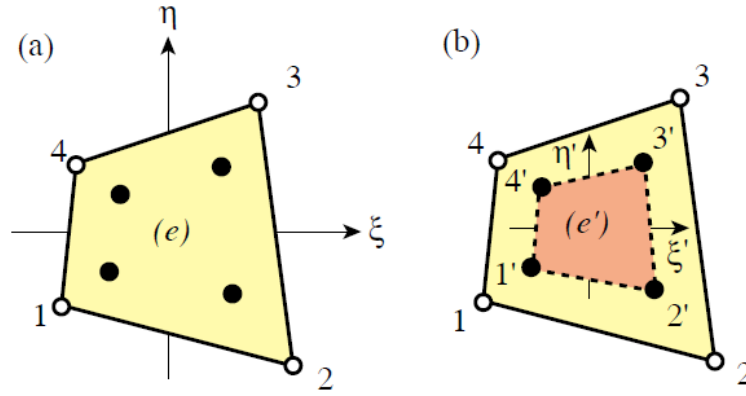


Fig (3.4) 4-node Gauss points: (a) 2x2 rule,(b) Gauss element

3.2.2 Stress-Strain relations:

In the two-dimensions the stresses and strain components are defined as (Akasha, 2009 and Mohamed et. el., 2013):

$$\{\varepsilon\} = \begin{Bmatrix} \varepsilon_x \\ \varepsilon_y \\ \gamma_{xy} \end{Bmatrix} \quad \text{For Green's strain} \quad (3.1)$$

Consider the material is an isotropic, the stresses are defined by:

$$\{\sigma\} = \begin{Bmatrix} \sigma_x \\ \sigma_y \\ \tau_{xy} \end{Bmatrix} = [D]\{\varepsilon\} \quad \text{For Green's strain} \quad (3.2)$$

Where D is elasticity matrix, in case of isotropic material,

$$[D] = \frac{E}{(1+\nu)(1-2\nu)} \begin{bmatrix} 1-\nu & \nu & 0 \\ \nu & 1-\nu & 0 \\ 0 & 0 & \frac{1-2\nu}{2} \end{bmatrix} \quad \text{For plane strain case} \quad (3.3a)$$

$$[D] = \frac{E}{1-\nu^2} \begin{bmatrix} 1 & \nu & 0 \\ \nu & 1 & 0 \\ 0 & 0 & \frac{1-\nu}{2} \end{bmatrix} \quad \text{For plane stress case} \quad (3.3b)$$

It is using the shape function for the geometry for defining the geometry at any point within the element in terms of nodal vectors as:

$$x = \sum_{i=1}^4 N_i x_i \quad , \quad y = \sum_{i=1}^4 N_i y_i \quad (3.4a)$$

$$\begin{Bmatrix} x \\ y \end{Bmatrix} = \begin{bmatrix} N_1 & 0 & N_2 & 0 & N_3 & 0 & N_4 & 0 \\ 0 & N_1 & 0 & N_2 & 0 & N_3 & 0 & N_4 \end{bmatrix} \begin{Bmatrix} x_1 \\ y_1 \\ x_2 \\ y_2 \\ x_3 \\ y_3 \\ x_4 \\ y_4 \end{Bmatrix} = [N]\{X^e\} \quad (3.4b)$$

Where the N_i the shape function element as:

$$N_1 = \frac{(1-r)(1-s)}{4}, N_2 = \frac{(1+r)(1-s)}{4}, N_3 = \frac{(1+r)(1+s)}{4}, N_4 = \frac{(1-r)(1+s)}{4} \quad (3.5)$$

since r and s are the natural coordinates.

The displacement at any point is defined in terms of nodal displacements as:

$$\begin{Bmatrix} u \\ v \end{Bmatrix} = \begin{bmatrix} N_1 & 0 & N_2 & 0 & N_3 & 0 & N_4 & 0 \\ 0 & N_1 & 0 & N_2 & 0 & N_3 & 0 & N_4 \end{bmatrix} \begin{Bmatrix} u_1 \\ v_1 \\ u_2 \\ v_2 \\ u_3 \\ v_3 \\ u_4 \\ v_4 \end{Bmatrix} = [N]\{d^e\} \quad (3.6)$$

The relation between the Cartesian and natural coordinates can be obtained using chain rule of partial differential as:

$$\begin{aligned} \frac{\partial N_i}{\partial r} &= \frac{\partial N_i}{\partial x} \frac{\partial x}{\partial r} + \frac{\partial N_i}{\partial y} \frac{\partial y}{\partial r} \\ \frac{\partial N_i}{\partial s} &= \frac{\partial N_i}{\partial x} \frac{\partial x}{\partial s} + \frac{\partial N_i}{\partial y} \frac{\partial y}{\partial s} \end{aligned} \quad \text{Or}$$

$$\begin{Bmatrix} \frac{\partial}{\partial r} \\ \frac{\partial}{\partial s} \end{Bmatrix} = \begin{Bmatrix} \frac{\partial x}{\partial r} & \frac{\partial y}{\partial r} \\ \frac{\partial x}{\partial s} & \frac{\partial y}{\partial s} \end{Bmatrix} \begin{Bmatrix} \frac{\partial}{\partial x} \\ \frac{\partial}{\partial y} \end{Bmatrix} = [J] \begin{Bmatrix} \frac{\partial}{\partial x} \\ \frac{\partial}{\partial y} \end{Bmatrix} \quad (3.7)$$

Where $[J]$ is Jacobian matrix

It relates derivatives of function in local coordinate system to derivative in global coordinate system which obtained by solving (3.7) as:

$$\begin{pmatrix} \frac{\partial}{\partial x} \\ \frac{\partial}{\partial y} \end{pmatrix} = [J]^{-1} \begin{pmatrix} \frac{\partial}{\partial r} \\ \frac{\partial}{\partial s} \end{pmatrix} \quad (3.8)$$

Since N_i is function in natural coordinates (r,s) the Jacobian matrix can be evaluated as:

$$[J^e] = \begin{bmatrix} \frac{\partial x}{\partial r} & \frac{\partial y}{\partial r} \\ \frac{\partial x}{\partial s} & \frac{\partial y}{\partial s} \end{bmatrix} = \begin{bmatrix} \sum_{i=1}^4 \frac{\partial N_i}{\partial r} x^e_i & \sum_{i=1}^4 \frac{\partial N_i}{\partial r} y^e_i \\ \sum_{i=1}^4 \frac{\partial N_i}{\partial s} x^e_i & \sum_{i=1}^4 \frac{\partial N_i}{\partial s} y^e_i \end{bmatrix}$$

$$[J] = \begin{bmatrix} \frac{\partial N_1}{\partial r} & \frac{\partial N_2}{\partial r} & \frac{\partial N_3}{\partial r} & \frac{\partial N_4}{\partial r} \\ \frac{\partial N_1}{\partial s} & \frac{\partial N_2}{\partial s} & \frac{\partial N_3}{\partial s} & \frac{\partial N_4}{\partial s} \end{bmatrix} \begin{bmatrix} x_1 & y_1 \\ x_2 & y_2 \\ x_3 & y_3 \\ x_4 & y_4 \end{bmatrix} \quad (3.9)$$

Using the values of N_i and substituting their derivatives in (3.9) to gives:

$$[J] = \begin{bmatrix} \frac{-(1-s)}{4} & \frac{(1-s)}{4} & \frac{(1+s)}{4} & \frac{-(1+s)}{4} \\ \frac{-(1-r)}{4} & \frac{-(1+r)}{4} & \frac{(1+r)}{4} & \frac{(1+r)}{4} \end{bmatrix} \begin{bmatrix} x_1 & y_1 \\ x_2 & y_2 \\ x_3 & y_3 \\ x_4 & y_4 \end{bmatrix} \quad (3.10)$$

$$\text{The inverse of Jacobin } [J]^{-1} = \begin{bmatrix} \frac{\partial r}{\partial x} & \frac{\partial s}{\partial x} \\ \frac{\partial r}{\partial y} & \frac{\partial s}{\partial y} \end{bmatrix} = \frac{1}{\det[J]} \begin{bmatrix} \frac{\partial y}{\partial r} & -\frac{\partial y}{\partial s} \\ -\frac{\partial x}{\partial r} & \frac{\partial x}{\partial s} \end{bmatrix}$$

$$[J]^{-1} = [J^*] = \begin{bmatrix} J^*_{11} & J^*_{12} \\ J^*_{21} & J^*_{22} \end{bmatrix}, \text{ where } \det [J] = \frac{\partial x}{\partial r} \times \frac{\partial y}{\partial s} - \frac{\partial y}{\partial r} \times \frac{\partial x}{\partial s}$$

And $J^*_{11}, J^*_{12}, J^*_{21}$ and J^*_{22} are the elements of Jacobin inverse matrix

The derivatives of displacement in Cartesian coordinates can be expressed in terms of natural coordinates as:

$$\begin{Bmatrix} \frac{\partial u}{\partial x} \\ \frac{\partial u}{\partial y} \\ \frac{\partial v}{\partial x} \\ \frac{\partial v}{\partial y} \end{Bmatrix} = \begin{bmatrix} J_{11}^* & J_{12}^* & 0 & 0 \\ J_{21}^* & J_{22}^* & 0 & 0 \\ 0 & 0 & J_{11}^* & J_{12}^* \\ 0 & 0 & J_{21}^* & J_{22}^* \end{bmatrix} \begin{Bmatrix} \frac{\partial u}{\partial r} \\ \frac{\partial u}{\partial s} \\ \frac{\partial v}{\partial r} \\ \frac{\partial v}{\partial s} \end{Bmatrix} \quad (3.11)$$

3.2.3 Incremental Formulations for Geometrically Nonlinear Plane Stress/Strain Element

The Green strains ε and their variation $\delta\varepsilon$ are defined in terms of the nodal variables in finite element representation as (Kim, 2014 and Bathe, et. el., 1975):

$$\{\varepsilon\} = \begin{Bmatrix} \varepsilon_x \\ \varepsilon_y \\ \gamma_{xy} \end{Bmatrix} = \begin{Bmatrix} \frac{\partial u}{\partial x} \\ \frac{\partial v}{\partial y} \\ \frac{\partial u}{\partial y} + \frac{\partial v}{\partial x} \end{Bmatrix} + \frac{1}{2} \begin{bmatrix} \frac{\partial u}{\partial x} & \frac{\partial v}{\partial y} & 0 & 0 \\ 0 & 0 & \frac{\partial u}{\partial y} & \frac{\partial v}{\partial x} \\ \frac{\partial u}{\partial y} & \frac{\partial v}{\partial y} & \frac{\partial u}{\partial x} & \frac{\partial v}{\partial x} \end{bmatrix} \begin{Bmatrix} \frac{\partial u}{\partial x} \\ \frac{\partial u}{\partial y} \\ \frac{\partial v}{\partial x} \\ \frac{\partial v}{\partial y} \end{Bmatrix} \quad (3.12)$$

$$\text{Or } \{\varepsilon\} = \{\varepsilon_0\} + \{\varepsilon_L\} \quad (3.13)$$

Where $\{\varepsilon_0\}$ is the linear strain vector, $\{\varepsilon_L\}$ is non-linear strain component

$$\text{Let } [A] = \begin{bmatrix} \frac{\partial u}{\partial x} & \frac{\partial v}{\partial y} & 0 & 0 \\ 0 & 0 & \frac{\partial u}{\partial y} & \frac{\partial v}{\partial x} \\ \frac{\partial u}{\partial y} & \frac{\partial v}{\partial y} & \frac{\partial u}{\partial x} & \frac{\partial v}{\partial x} \end{bmatrix} \quad (3.14)$$

Where $[A]$ is the matrix containing displacement derivatives w. r. t Cartesian coordinates

And

$$\{\theta\} = \begin{Bmatrix} \frac{\partial u}{\partial x} \\ \frac{\partial u}{\partial y} \\ \frac{\partial v}{\partial x} \\ \frac{\partial v}{\partial y} \end{Bmatrix} \quad (3.15)$$

Where:

$\{\theta\}$ Is vector containing displacement derivatives *w.r.t.* Cartesian Coordinates.

Then the non-linear strain is:

$$\{\varepsilon_L\} = \frac{1}{2}[A]\{\theta\} \quad (3.16)$$

The displacements are defined in terms of nodal parameters using the appropriate shape functions, thus

$$u = \sum_{i=1}^4 N_i u_i \quad \text{and} \quad v = \sum_{i=1}^4 N_i v_i \quad \text{or} \quad \begin{Bmatrix} u \\ v \end{Bmatrix} = [N]\{a\} \quad (3.17)$$

And there derivatives:

$$\{\theta\} = [G]\{a\} \quad (3.18)$$

Where:

$$\{a\} = [u_1 \quad v_1 \quad u_2 \quad v_2 \quad u_3 \quad v_3 \quad u_4 \quad v_4]^T \quad (3.19)$$

Is vector of nodal displacements and:

$$[G] = \begin{bmatrix} \frac{\partial N_1}{\partial x} & 0 & \frac{\partial N_2}{\partial x} & 0 & \frac{\partial N_3}{\partial x} & 0 & \frac{\partial N_4}{\partial x} & 0 \\ \frac{\partial N_1}{\partial y} & 0 & \frac{\partial N_2}{\partial y} & 0 & \frac{\partial N_3}{\partial y} & 0 & \frac{\partial N_4}{\partial y} & 0 \\ 0 & \frac{\partial N_1}{\partial x} & 0 & \frac{\partial N_2}{\partial x} & 0 & \frac{\partial N_3}{\partial x} & 0 & \frac{\partial N_4}{\partial x} \\ 0 & \frac{\partial N_1}{\partial y} & 0 & \frac{\partial N_2}{\partial y} & 0 & \frac{\partial N_3}{\partial y} & 0 & \frac{\partial N_4}{\partial y} \end{bmatrix} \quad (3.20)$$

$[G]$ Is the matrix containing shape function derivatives *w.r.t.* Cartesian coordinates.

From equations (3.12) and (3.17) $\{\varepsilon_0\}$ can be obtained as:

$$\{\varepsilon_0\} = \begin{Bmatrix} \frac{\partial u}{\partial x} \\ \frac{\partial v}{\partial y} \\ \frac{\partial u}{\partial y} + \frac{\partial v}{\partial x} \end{Bmatrix} = \begin{bmatrix} \frac{\partial}{\partial x} & 0 \\ 0 & \frac{\partial}{\partial y} \\ \frac{\partial}{\partial y} & \frac{\partial}{\partial x} \end{bmatrix} \begin{Bmatrix} u \\ v \end{Bmatrix} \quad (3.21)$$

$$\text{or } \{\varepsilon_0\} = [B_0]\{a\}$$

In the Total Lagrangian formulations, the infinitesimal strain-displacement transformation $[B_0]$ becomes (Kim, 2014 and Bathe, et. el., 1975):

$$[B_0] = \begin{bmatrix} \frac{\partial N_1}{\partial x} & 0 & \frac{\partial N_2}{\partial x} & 0 & \frac{\partial N_3}{\partial x} & 0 & \frac{\partial N_4}{\partial x} & 0 \\ 0 & \frac{\partial N_1}{\partial y} & 0 & \frac{\partial N_{21}}{\partial y} & 0 & \frac{\partial N_3}{\partial y} & 0 & \frac{\partial N_3}{\partial y} \\ \frac{\partial N_1}{\partial y} & \frac{\partial N_1}{\partial x} & \frac{\partial N_2}{\partial y} & \frac{\partial N_2}{\partial x} & \frac{\partial N_3}{\partial y} & \frac{\partial N_3}{\partial x} & \frac{\partial N_4}{\partial y} & \frac{\partial N_4}{\partial x} \end{bmatrix} \quad (3.22)$$

Taking the variation of equation (3.16) gives:

$$\delta\{\varepsilon_L\} = \frac{1}{2}[A]\delta\{\theta\} + \frac{1}{2}[A]\delta\{\theta\} = [A]\delta\{\theta\} = [A][G]\delta\{a\} = [B_L]\delta\{a\} \quad (3.23)$$

In which

$$[B_L] = [A][G] \quad \text{Or}$$

The linear strain matrix $[B_L]$ in total Lagrangian formulation becomes (Kim, 2014 and Bathe, et .el., 1975):

$$[B_L] = \begin{bmatrix} F_{11} \frac{\partial N_1}{\partial x} & F_{21} \frac{\partial N_1}{\partial x} & F_{11} \frac{\partial N_2}{\partial x} & F_{21} \frac{\partial N_2}{\partial x} & F_{11} \frac{\partial N_3}{\partial x} & F_{21} \frac{\partial N_3}{\partial x} & F_{11} \frac{\partial N_4}{\partial x} & F_{21} \frac{\partial N_4}{\partial x} \\ F_{12} \frac{\partial N_1}{\partial y} & F_{22} \frac{\partial N_1}{\partial y} & F_{12} \frac{\partial N_2}{\partial y} & F_{22} \frac{\partial N_2}{\partial y} & F_{12} \frac{\partial N_3}{\partial y} & F_{22} \frac{\partial N_3}{\partial y} & F_{12} \frac{\partial N_4}{\partial y} & F_{22} \frac{\partial N_4}{\partial y} \\ (F_{11} \frac{\partial N_1}{\partial y} & (F_{21} \frac{\partial N_1}{\partial y} & (F_{11} \frac{\partial N_2}{\partial y} & (F_{21} \frac{\partial N_2}{\partial y} & (F_{11} \frac{\partial N_3}{\partial y} & (F_{21} \frac{\partial N_3}{\partial y} & F_{11} \frac{\partial N_4}{\partial y} & F_{21} \frac{\partial N_4}{\partial y} \\ +F_{12} \frac{\partial N_1}{\partial x}) & +F_{22} \frac{\partial N_1}{\partial x}) & +F_{12} \frac{\partial N_2}{\partial x}) & +F_{22} \frac{\partial N_2}{\partial x}) & +F_{12} \frac{\partial N_3}{\partial x}) & +F_{22} \frac{\partial N_3}{\partial x}) & +F_{12} \frac{\partial N_4}{\partial x}) & +F_{22} \frac{\partial N_4}{\partial x}) \end{bmatrix} \quad (3.24)$$

Where $\{F_{ij}\}$ is the deformation gradient vector which can be written as:

$$\{F\} = \{F_{11} \ F_{12} \ F_{21} \ F_{22}\}^T = \left\{1 + \frac{\partial u}{\partial x} \quad \frac{\partial u}{\partial y} \quad \frac{\partial v}{\partial x} \quad 1 + \frac{\partial v}{\partial y}\right\}^T \quad (3.25)$$

Using equations (3.22) and (3.23) and taking the variation of equation (3.13) gives:

$$\delta\{\varepsilon\} = [B_0]\delta\{a\} + [B_L]\delta\{a\} = ([B_0] + [B_L])\delta\{a\} = [B]\delta\{a\} \quad (3.26)$$

In which

$$[B] = [B_0] + [B_L] \quad (3.27)$$

3.3 Formulation of Geometrically Nonlinear Plane Stress/Strain Element:

In this section the 2nd Piola-Kirchhoff stresses and the Green Lagrangian strain are used in total Lagrangian formulations. The solution of the resulting nonlinear equations is obtained by incremental and Newton-Raphson method.

3.3.1 Stress-Strain relations

$$[\sigma] = \begin{Bmatrix} \sigma_x \\ \sigma_y \\ \tau_{xy} \end{Bmatrix} = [D] \begin{Bmatrix} \varepsilon_x \\ \varepsilon_y \\ \gamma_{xy} \end{Bmatrix} \quad \text{or} \quad [D]\{\varepsilon\} \quad (3.28)$$

Where $[D]$ is given by (3.3) for plane stress and plane strain.

For Green's strain and 2nd Piola-Kirchhoff stresses

3.3.2 Strain-Displacement Relations:

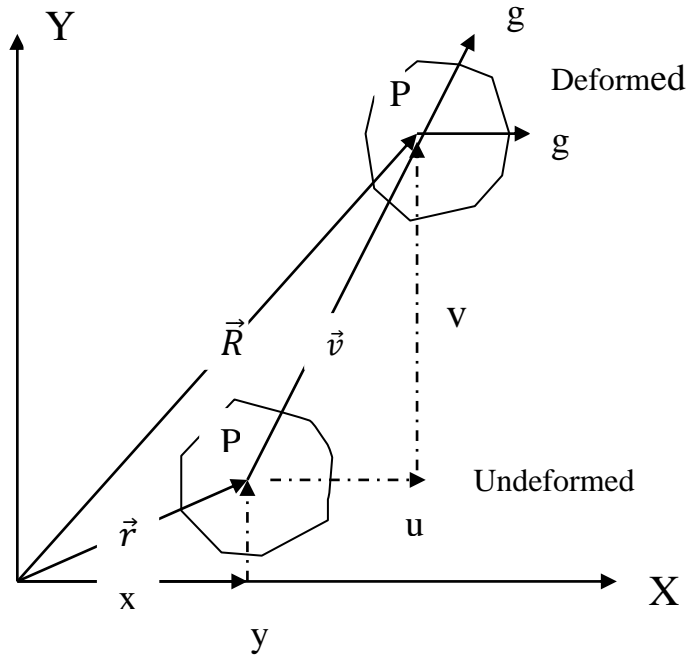


Fig (3.5) Deformed and Undeformed shape

Referring to Fig (3.4), the position vector for point $P(x, y)$ after deformation is:

$$\vec{R} = (x + u)\mathbf{i} + (y + v)\mathbf{j} \quad (3.29)$$

In which u and v are components of displacement in the global axes directions

The displacement gradient vectors are given from equation (3.29) by:

$$\vec{g}_x = \frac{\partial \vec{R}}{\partial x} = \left(1 + \frac{\partial u}{\partial x}\right)\mathbf{i} + \frac{\partial v}{\partial x}\mathbf{j}$$

$$\vec{g}_y = \frac{\partial \vec{R}}{\partial y} = \left(\frac{\partial u}{\partial y}\right)\mathbf{i} + \left(1 + \frac{\partial v}{\partial y}\right)\mathbf{j} \quad (3.30)$$

3.3.3 Green Lagrangian Strain

The Green's strains are defined by a vector:

$$\{\varepsilon\} = \begin{Bmatrix} \varepsilon_x \\ \varepsilon_y \\ \gamma_{xy} \end{Bmatrix} = \begin{Bmatrix} \frac{1}{2}(\mathbf{g}_x \cdot \mathbf{g}_x - 1) \\ \frac{1}{2}(\mathbf{g}_y \cdot \mathbf{g}_y - 1) \\ \mathbf{g}_x \cdot \mathbf{g}_y \end{Bmatrix} \quad (3.31)$$

From equation (3.30)

$$\begin{aligned} \mathbf{g}_x \cdot \mathbf{g}_x &= \left[\left(1 + \frac{\partial u}{\partial x}\right) i + \frac{\partial v}{\partial x} j \right] \cdot \left[\left(1 + \frac{\partial u}{\partial x}\right) i + \frac{\partial v}{\partial x} j \right] = \left(1 + \frac{\partial u}{\partial x}\right)^2 + \left(\frac{\partial v}{\partial x}\right)^2 \\ &= 1 + 2 \frac{\partial u}{\partial x} + \left(\frac{\partial u}{\partial x}\right)^2 + \left(\frac{\partial v}{\partial x}\right)^2 \end{aligned}$$

Similarly:

$$\begin{aligned} \mathbf{g}_y \cdot \mathbf{g}_y &= \left[\left(\frac{\partial u}{\partial y}\right) i + \left(1 + \frac{\partial v}{\partial y}\right) j \right] \cdot \left[\left(\frac{\partial u}{\partial y}\right) i + \left(1 + \frac{\partial v}{\partial y}\right) j \right] = \left(\frac{\partial u}{\partial y}\right)^2 + \left(1 + \frac{\partial v}{\partial y}\right)^2 \\ &= 1 + 2 \frac{\partial v}{\partial y} + \left(\frac{\partial v}{\partial y}\right)^2 + \left(\frac{\partial u}{\partial y}\right)^2 \end{aligned}$$

And

$$\begin{aligned} \mathbf{g}_x \cdot \mathbf{g}_y &= \left[\left(1 + \frac{\partial u}{\partial x}\right) i + \frac{\partial v}{\partial x} j \right] \cdot \left[\left(\frac{\partial u}{\partial y}\right) i + \left(1 + \frac{\partial v}{\partial y}\right) j \right] \\ &= \left(1 + \frac{\partial u}{\partial x}\right) \frac{\partial u}{\partial y} + \frac{\partial v}{\partial x} \left(1 + \frac{\partial v}{\partial y}\right) \\ &= \frac{\partial u}{\partial y} + \frac{\partial u}{\partial y} \frac{\partial u}{\partial x} + \frac{\partial v}{\partial x} + \frac{\partial v}{\partial x} \frac{\partial v}{\partial y} \\ &= \frac{\partial u}{\partial y} + \frac{\partial v}{\partial x} + \frac{\partial u}{\partial y} \frac{\partial u}{\partial x} + \frac{\partial v}{\partial x} \frac{\partial v}{\partial y} \end{aligned}$$

Substituting in equation (3.31) the strains become:

$$\{\varepsilon\} = \begin{Bmatrix} \varepsilon_x \\ \varepsilon_y \\ \gamma_{xy} \end{Bmatrix} = \begin{Bmatrix} \frac{\partial u}{\partial x} + \frac{1}{2} \left(\frac{\partial u}{\partial x}\right)^2 + \frac{1}{2} \left(\frac{\partial v}{\partial x}\right)^2 \\ \frac{\partial v}{\partial y} + \frac{1}{2} \left(\frac{\partial v}{\partial y}\right)^2 + \frac{1}{2} \left(\frac{\partial u}{\partial y}\right)^2 \\ \frac{\partial u}{\partial y} + \frac{\partial v}{\partial x} + \frac{\partial u}{\partial y} \frac{\partial u}{\partial x} + \frac{\partial v}{\partial x} \frac{\partial v}{\partial y} \end{Bmatrix} \quad (3.32)$$

3.3.4 Tangent Stiffness Matrix due to Green Strains:

From virtual work, the equilibrium equations can be written as:

$$\{\varphi\} = \int_v [B]^T \{\sigma\} dv - \{f\} = 0 \quad (3.33)$$

Where:

$\{\varphi\}$ Is the difference between external and internal generalized forces

$\{f\}$ Is the vector of external forces

$\{\sigma\}$ Is the 2nd Piola-Kirchhoff stresses vector

The stiffness matrix is obtained by taking the variation of equation (3.33) w.r.t the nodal variables $\{a\}$

$$\delta\{\varphi\} = \int_v [B]^T \delta\{\sigma\} dv + \int_v \delta[B]^T \{\sigma\} dv \quad (3.34)$$

The discretized element of volume $dv = h \det J dr ds$

Where h Is the thickness of the element

Using equation (3.26) and (3.24)

$$\{\sigma\} = \begin{Bmatrix} \sigma_x \\ \sigma_y \\ \tau_{xy} \end{Bmatrix} = [D] \begin{Bmatrix} \varepsilon_x \\ \varepsilon_y \\ \gamma_{xy} \end{Bmatrix} \quad or \quad \{\sigma\} = [D]\{\varepsilon\}$$

And

$$\delta\{\sigma\} = [D]\delta\{\varepsilon\} = [D][B]\delta\{a\}$$

$$\text{Therefore } \int_v [B]^T \delta\{\sigma\} dv = \left(\int_v [B]^T [D][B] dv \right) \delta\{a\} = ([K_0] + [K_L])\delta\{a\} \quad (3.35)$$

Where the matrix $[K_0]$ represents to the small displacement stiffness matrix and is given by:

$$[K_0] = \int [B_0]^T [D] [B_0] dv \quad (3.36)$$

And the matrix $[K_L] = \int ([B_0]^T [D] [B_L] + [B_L]^T [D] [B_0] + [B_L] [D] [B_L]) dv$

$$(3.37)$$

Where $[K_L]$ Is the linear strain stiffness matrix

From equation (3.25)

$$[B]^T = [B_0]^T + [B_L]^T$$

By taking the variation of $[B]^T$ and using equation (3.23) we have:

$$\delta[B]^T = \delta[B_L]^T = [G]^T \delta[A]^T$$

Therefore

$$\int_v \delta[B]^T \{\sigma\} dv = \int_v [G]^T \delta[A]^T \{\sigma\} dv = [K_\sigma] \delta\{a\}$$

$$(3.38)$$

Where $[K_\sigma]$ is a symmetric matrix depending on the stress level and is known as the initial stress matrix

Using equations (3.26), (3.14) & (3.18)

$$\begin{aligned}
[A]^T\{\sigma\} &= \begin{bmatrix} \frac{\partial u}{\partial x} & 0 & \frac{\partial u}{\partial y} \\ \frac{\partial v}{\partial x} & 0 & \frac{\partial v}{\partial y} \\ 0 & \frac{\partial u}{\partial y} & \frac{\partial u}{\partial x} \\ 0 & \frac{\partial v}{\partial y} & \frac{\partial v}{\partial x} \end{bmatrix} \begin{Bmatrix} \sigma_x \\ \sigma_y \\ \gamma_{xy} \end{Bmatrix} = \begin{bmatrix} \frac{\partial u}{\partial x} \sigma_x + \frac{\partial u}{\partial y} \gamma_{xy} \\ \frac{\partial v}{\partial x} \sigma_x + \frac{\partial v}{\partial y} \gamma_{xy} \\ \frac{\partial u}{\partial y} \sigma_y + \frac{\partial u}{\partial x} \gamma_{xy} \\ \frac{\partial v}{\partial y} \sigma_y + \frac{\partial v}{\partial x} \gamma_{xy} \end{bmatrix} \\
&= \begin{bmatrix} \sigma_x & 0 & \gamma_{xy} & 0 \\ 0 & \sigma_x & 0 & \gamma_{xy} \\ \gamma_{xy} & 0 & \sigma_y & 0 \\ 0 & \gamma_{xy} & 0 & \sigma_y \end{bmatrix} \begin{Bmatrix} \frac{\partial u}{\partial x} \\ \frac{\partial u}{\partial y} \\ \frac{\partial v}{\partial x} \\ \frac{\partial v}{\partial y} \end{Bmatrix}
\end{aligned}$$

$$\text{Or } [A]^T\{\sigma\} = [M]\{\theta\} = [M][G]\{a\} \quad (3.39)$$

Where $[M]$ is initial stress matrix and is given by:

$$[M] = \begin{bmatrix} \sigma_x[I] & \tau_{xy}[I] \\ \tau_{xy}[I] & \sigma_y[I] \end{bmatrix}, [I] = \begin{bmatrix} 1 & 0 \\ 0 & 1 \end{bmatrix} \quad (3.40)$$

Taking the variation of Eq. (3.39) gives

$$\delta[A]^T\{\sigma\} = [M][G]\delta\{a\} \quad (3.41)$$

Substitute equation (3.40) in (3.38) to get:

$$\int_v [G]^T \delta[A]^T\{\sigma\} dv = \left(\int_v [G]^T [M]\{G\} dv \right) \delta\{a\} = [K_\sigma]\delta\{a\} \quad (3.42)$$

$$\text{Therefore, } [K_\sigma] = \int_v [G]^T [M][G] dv \quad (3.43)$$

Where $[G]$ is the Non-linear strain-displacement transformation matrix written as:

$$[G] = \begin{bmatrix} \frac{\partial N_1}{\partial x} & 0 & \frac{\partial N_2}{\partial x} & 0 & \frac{\partial N_3}{\partial x} & 0 & \frac{\partial N_4}{\partial x} & 0 \\ \frac{\partial N_1}{\partial y} & 0 & \frac{\partial N_2}{\partial y} & 0 & \frac{\partial N_3}{\partial y} & 0 & \frac{\partial N_4}{\partial y} & 0 \\ 0 & \frac{\partial N_1}{\partial x} & 0 & \frac{\partial N_2}{\partial x} & 0 & \frac{\partial N_3}{\partial x} & 0 & \frac{\partial N_4}{\partial x} \\ 0 & \frac{\partial N_1}{\partial y} & 0 & \frac{\partial N_2}{\partial y} & 0 & \frac{\partial N_3}{\partial y} & 0 & \frac{\partial N_4}{\partial y} \end{bmatrix} \quad (3.44)$$

From equations (3.35), (3.38) & (3.34)

$$\delta\{\varphi\} = ([K_0] + [K_L] + [K_\sigma])\delta\{a\} = [K_T]\delta\{a\}$$

Where:

$$[K_T] = [K_0] + [K_L] + [K_\sigma] \quad (3.45)$$

Is the total tangent stiffness matrix

3.4 Incremental Equilibrium Equations

From equation (3.45) the tangent stiffness matrix takes the form:

$$[K_T] = [K_0] + [K_L(a_0)] + [K_\sigma]$$

Where:

$$[K_0] + [K_L(a_0)] = \int_v [B]^T [D] [B] dv \quad (3.46)$$

$$[K_\sigma] = \int_v [G]^T [M] [G] dv \quad (3.47)$$

The displacement increments $\{\Delta a_0^i\}$ are evaluated by using $[K_T]$ and residuals as:

$$\{\Delta a_0^i\} = -[K_T]^{-1}\{\varphi\}^i \quad (3.48)$$

The strain increments are defined by:

$$\{\Delta \varepsilon\}^i = \left[[B_0] + [B_L(a_0^i)] + \frac{1}{2} [B_L(\Delta a_0^i)] \right] \{\Delta a_0^i\} \quad (3.49)$$

The stresses increments are given by:

$$\{\Delta S_0^i\} = [D]\{\Delta \varepsilon_0^i\} \quad (3.50)$$

The total stresses are:

$$\{S_0^{i+1}\} = \{S_0^i\} + \{\Delta S_0^i\} \quad (3.51)$$

The nodal residual forces for the next iteration are evaluated as follows:

$$\{-\varphi^{i+1}\} = \{R\} - \int_v [B]^T \{S^{i+1}\} dv \quad (3.52)$$

And

$$[B] = [B_0] + [B_L(a_0^{i+1})] \quad (3.53)$$

Chapter four

Implementation and Application of Program and Verification of Results

4.1 Description of Computer Program

4.1.1 Introduction

A computer program for linear and nonlinear analysis of plane stresses and plane strains by finite element method is presented in this chapter. The program was developed and written by MATLAB program language. The programs have nine subroutines or functions. The basic functions are, LINA2D and NONLA2D. The function LINA2D was developed for linear formulation, and the NONLA2D was developed for nonlinear formulation based on Green strain presented in chapter three.

The formulation stated in chapter three, was implemented in the standard MATLAB (2010b), and the major goals were to achieve good results, and compare them with known results. In the program the 4-noded 2-dimensional isoparametric element was used.

The main program procedures and the all functions are explained in the following sections, the listing of the main program and the subroutines are presented in Appendices A and B.

4.1.2 Main program procedures:

The basic stages of implementation of MATLAB programming are as follows:

- 1- read input data which include:
 - Mesh generation function
 - Element external nodal force EXTFORCE

- Material properties (Poisson ratio, Elastic modulus)
 - Program parameters (ITER, TOL, INC)
 - Load increments (Start increment, End increment ...)
 - Boundary conditions
- 2- Call FORD to calculate elastic modulus matrix [D]
 - 3- Read SHAPLE to compute shape functions, their derivatives and determinant of Jacobian of 4-noded element
 - 4- Before incrementing and Newton-Raphson iteration start, the main function/ program calls CHECK to check the area and connectivity of the elements and the program stops if the determinant is negative or if there is any error in the element connectivity.
 - 5- Begin load increments INC=1, and iteration ITER=1 for nonlinear analysis.
 - 6- If Anatype =1, call LINA2D to calculate element stiffness matrix and assemble it in global matrix for linear analysis.
 - 7- Else if Anatype is not equal to one use NONLINA2D to compute global tangent stiffness matrix KT, and residual force (FORCE) for nonlinear analysis.
 - 8- After calculation of KT and FORCE:

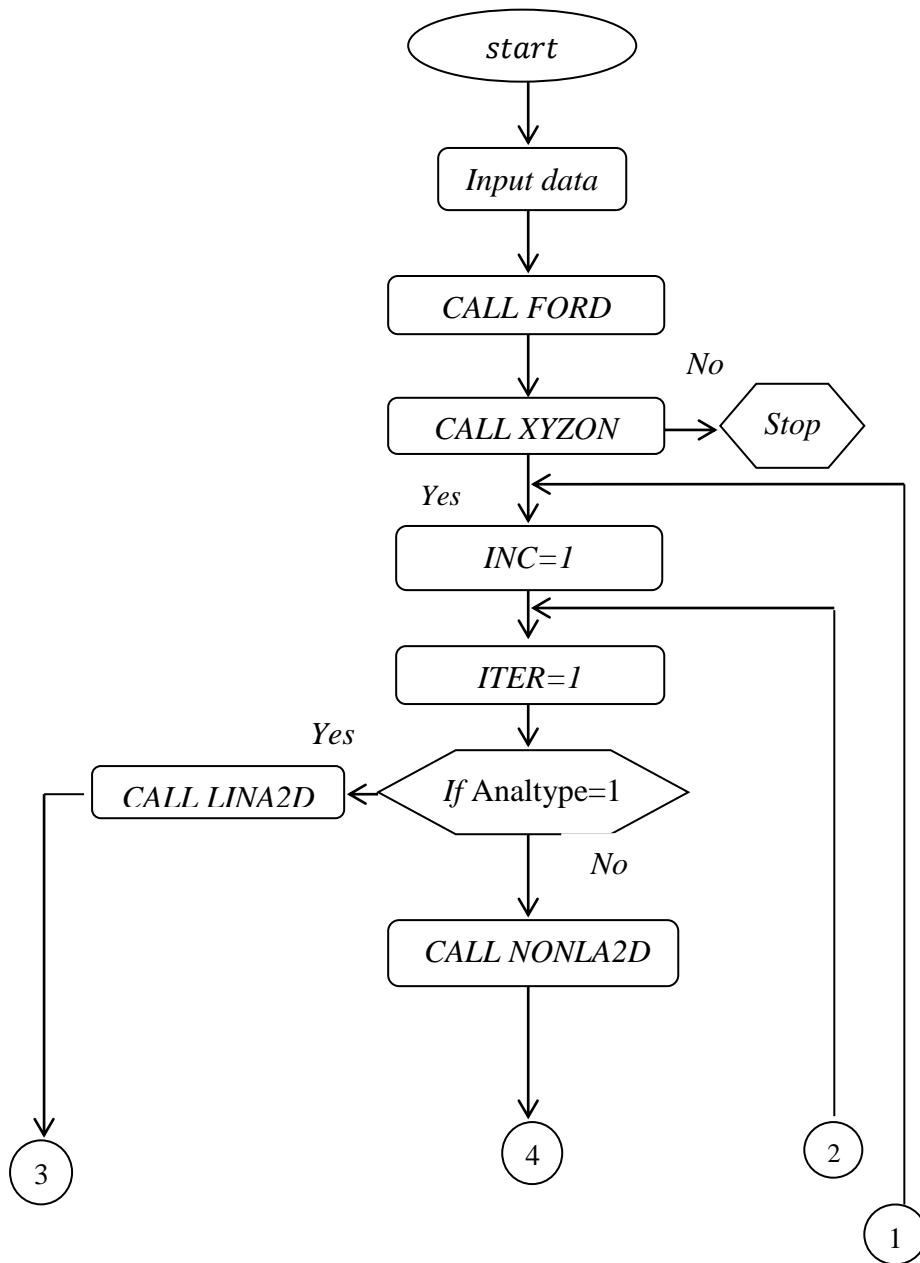
calculat:

- displacement increments $\Delta\{U\} = [K]^{-1}\{R\}$
- total displacement vector $\{U\} = \{U\} + \Delta\{U\}$
- strain increments
- stresses increments
- the total stresses
- the total residual force

- a- If solution has not converged or this is not the last iteration then go to next iteration (go to 5).
 - b- Else continue if solution has converged.
- 9- call OUTPUT print convergent results
- 10-call PROUT to print out convergence displacement and stresses
- 11-calculate direct stresses and shear stresses at integration points of elements
- 12 – If this is not the last increment go to (5); otherwise:
- 13- End program

4.1.3 Program layout

The computer program system is divided into main nine functions/ subroutines; each function consists of specific task in the program. The main program flow chart is shown in the Figure (4.1) and the subroutines are explained in the next section.



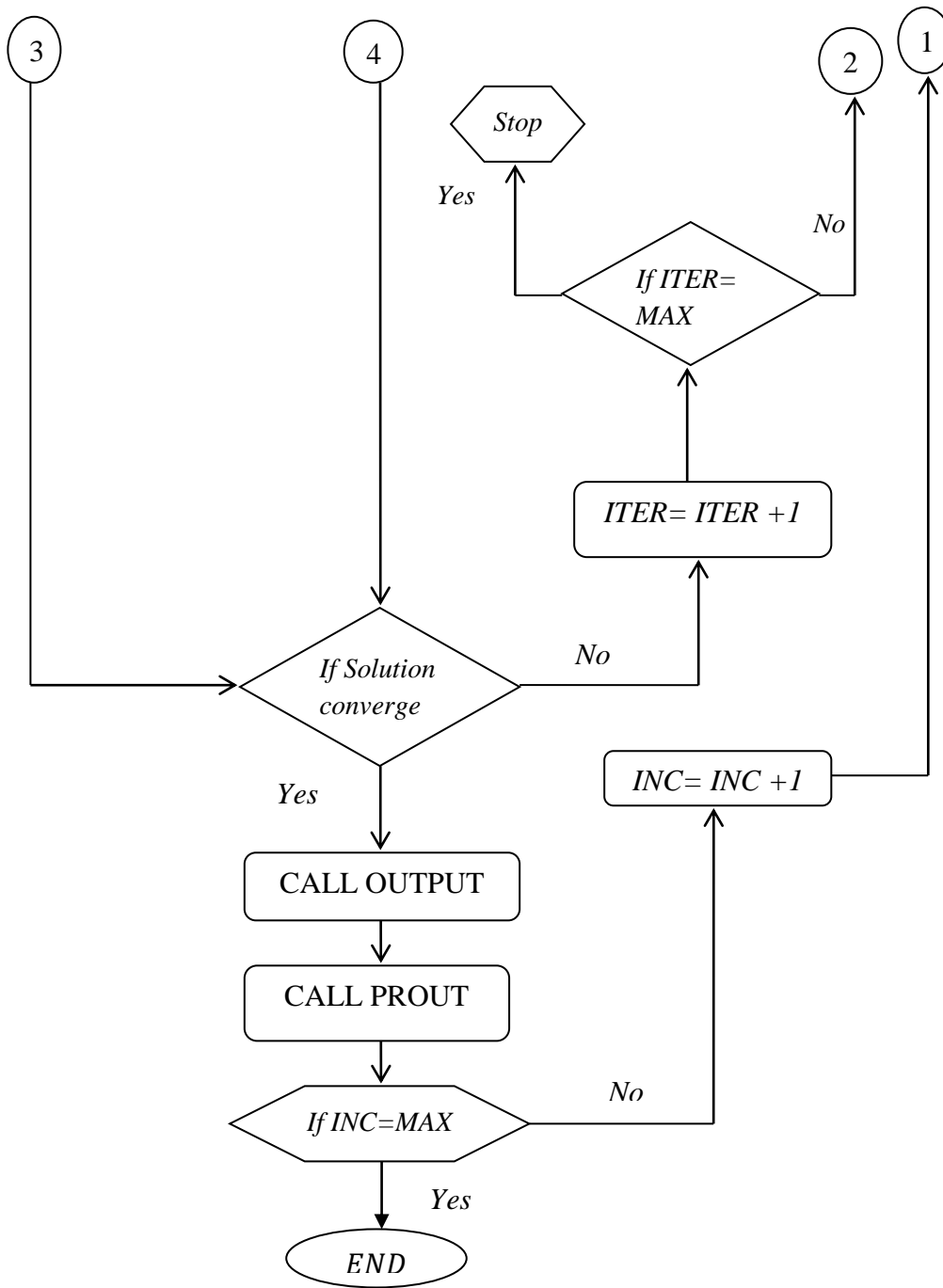
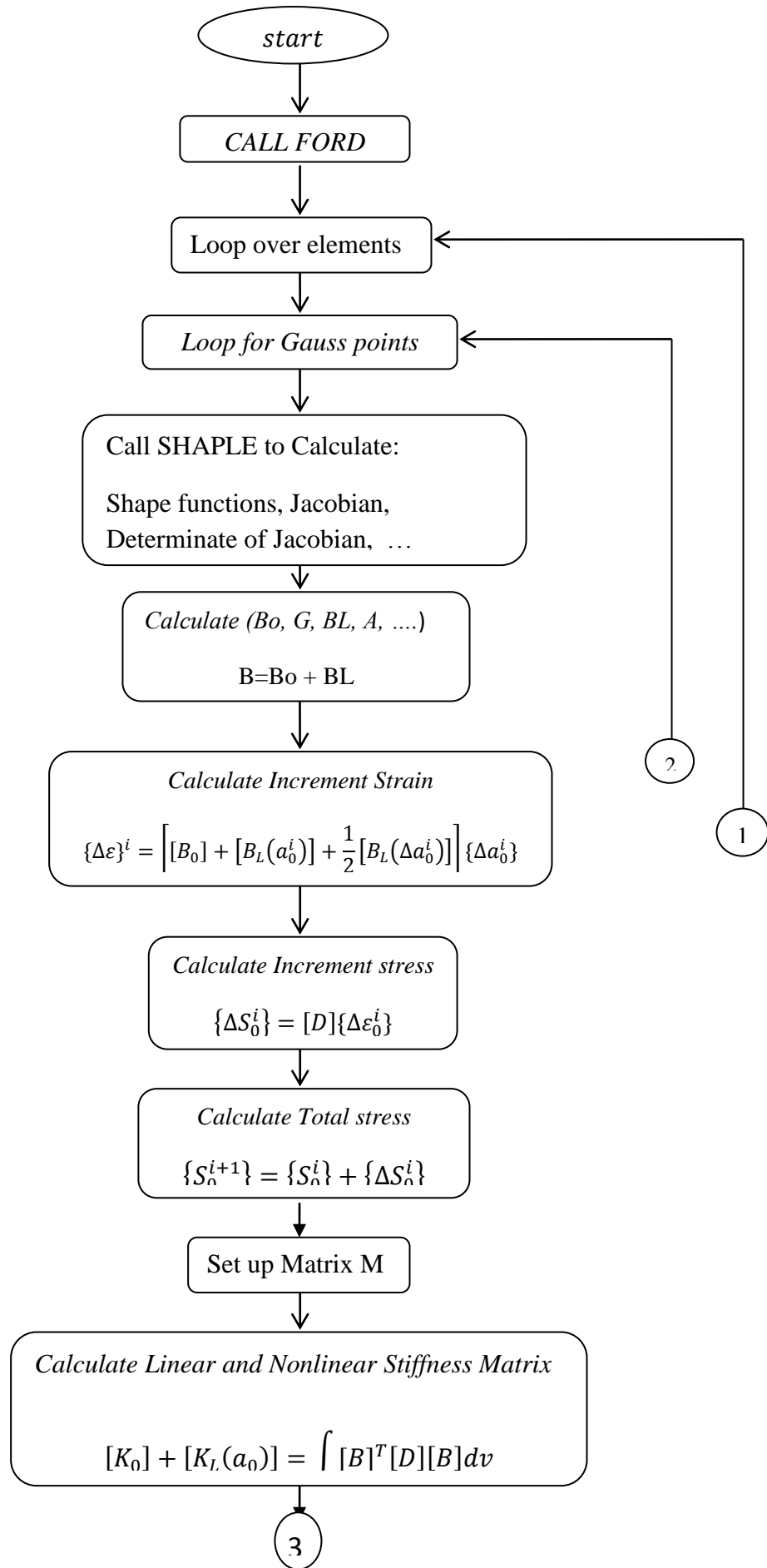


Fig (4.1) Main program flow chart



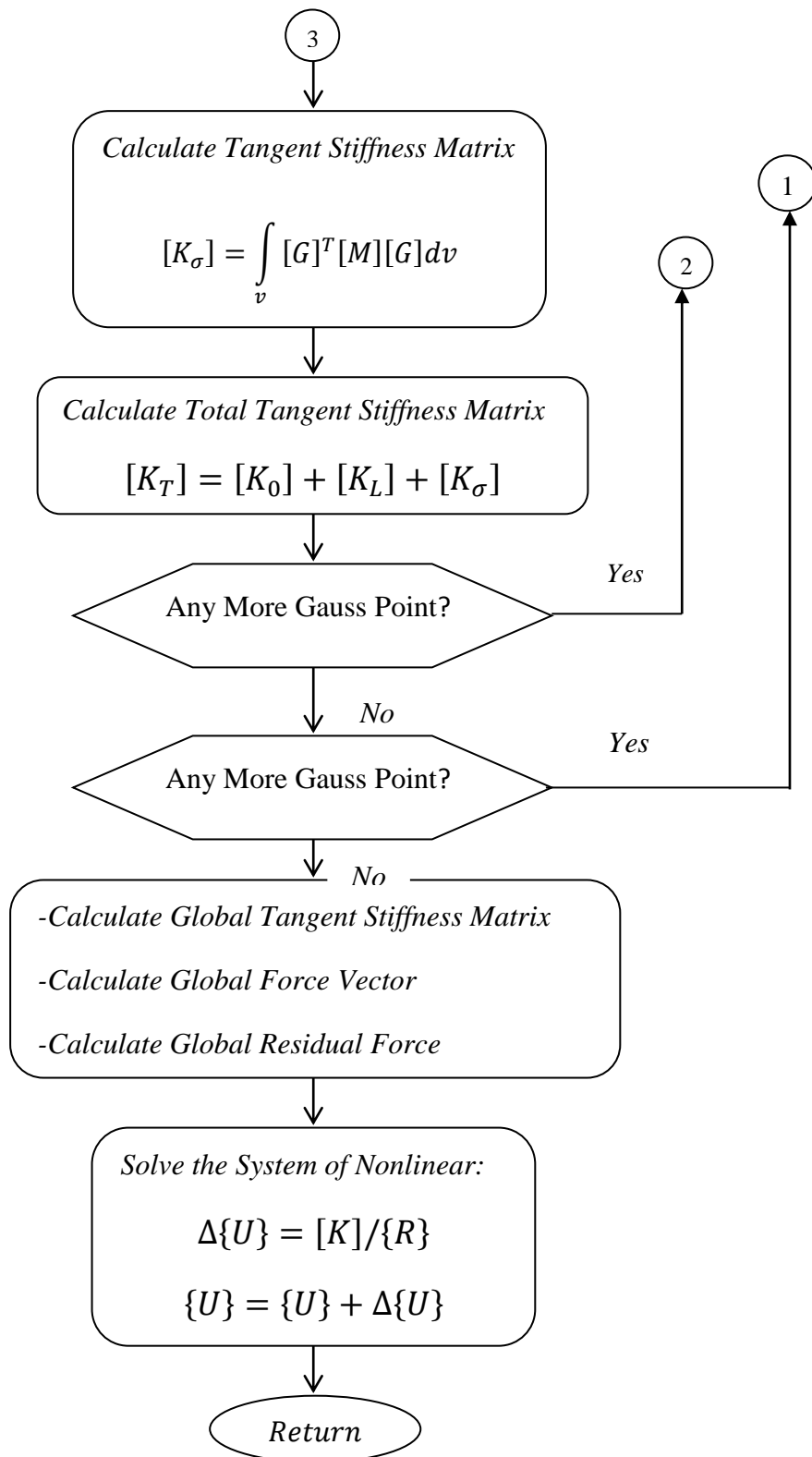


Fig (4.1a) flow chart for function NONLA2D

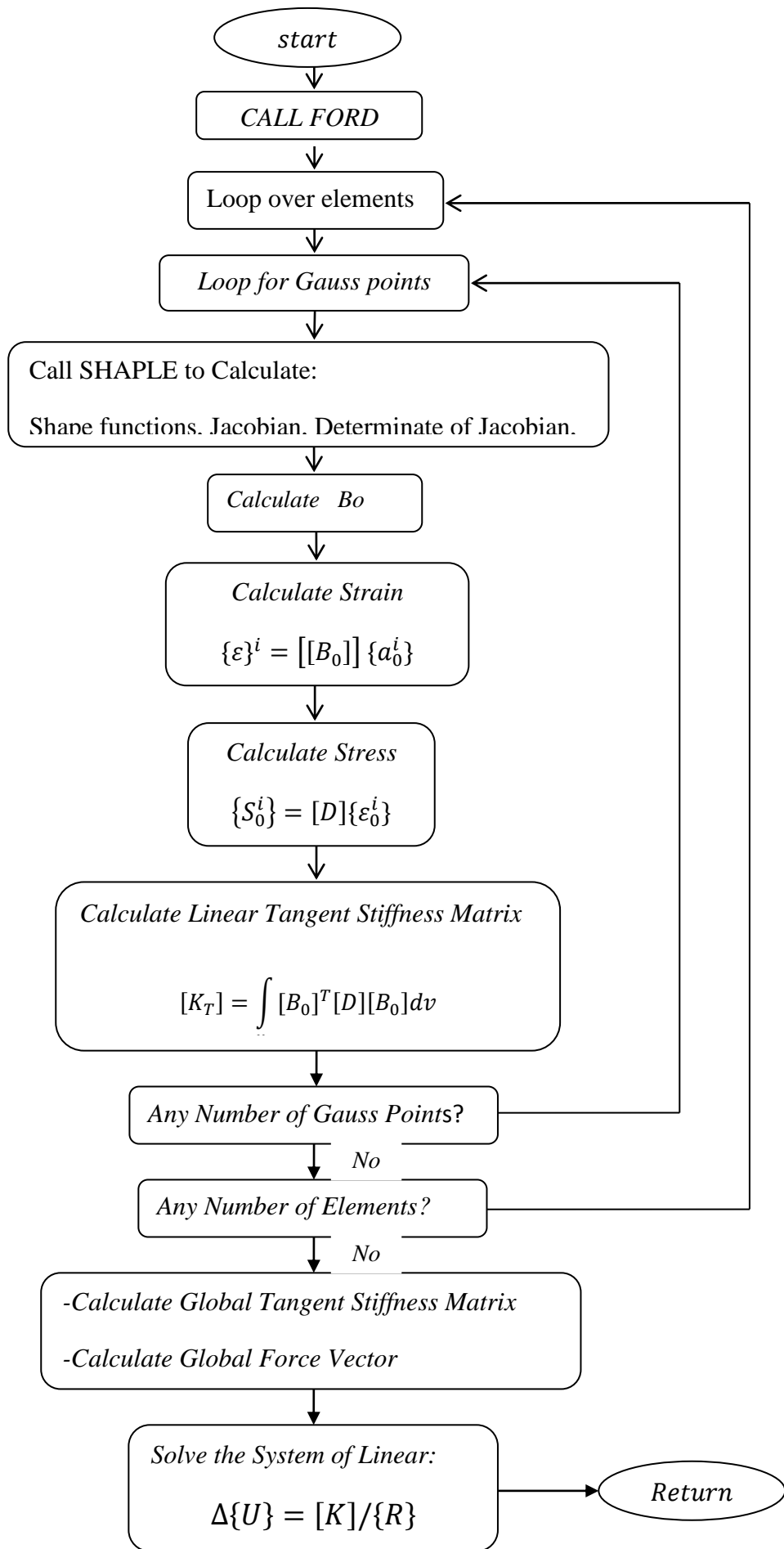


Fig (4.1b) flow chart of function LINA2D

4.1.4 Functions Explanation

1- Input data function

This subroutine consists of the basic data that is required in defining the geometry of 4-noded isoparametric element, connectivity, properties of element, and boundary conditions, external nodal force. It also reads the control parameters.

2- Function MESH

According to dimensions of the structure and specified sub-divisions in the two directions, this subroutine generates a mesh of linear quadrilateral elements.

3- Function FORD

This subroutine calculates the modulus matrix for linear elastic material [D]

4-Function SHAPLE

According to the 4-node isoparametric element, the function computes the shape functions, their derivatives, and determinant of the Jacobian of bilinear element.

5- CHECK function

This subroutine checks the determinant of element Jacobian matrix, and the program stops if the determinant is negative, which indicates that either element has negative area or the element connectivity is not correct.

6- LINA2D function

This is the main function for linear analysis as shown in Fig (4.1b), which starts when $Anatype = 1$. According to the integration point and weights, function reads the element nodal coordinate and calls the subroutine SHAPLE , FORD, to assemble the strain stiffness matrix and then assemble global stiffness matrix and Global force of linear elastic analysis. The function also calculate the

strain and stresses at integration points, and solve the system of linear analysis to compute the displacements at nodes.

7- NONLIA2D function

The function NONLA2D as shown in Fig (4.1a) is used to compute or assemble the global tangent stiffness matrix and residual force for nonlinear analysis, and solve the nonlinear equation to calculate the increment displacements, displacements, strain increments, stress increments and total stresses. The function starts when Analyte equals any number other than one.

8- OUTPUT function

This function is prints out iteration of results to MATLAB screen.

9- PROUT function

This function prints out analysis results.

4.2 Verification of Formulation

4.2.1 Introduction

For the linear and nonlinear analyses three numerical examples of large deformation problems were analysed to demonstrate the degree of accuracy that can be obtained by using the linear and the geometrically nonlinear formulation based on Green strain and 4-node plane stress/strain element.

The result of displacements, stresses at the integration points and the differences between incremental displacements and incremental stresses are obtained and compared with known results.

4.2.2 Linear analysis

4.2.2.1 Cantilever plate under concentrated load at the end

The linear formulation was tested by analyzing the cantilever plate beam subjected to load at free end. The cantilever is of dimension $L=3000\text{mm}$, $D=300\text{mm}$ and thickness $h=60\text{mm}$ as shown in Fig (4.2). The numerical values of material property parameter are: Young's modulus $E=210 \times 10^3 \text{ N/mm}^2$, Poisson's ratio $\nu = 0.3$. The structure is modeled with different numbers of isoparametric elements. The result obtained for displacements and stresses are compared with known results. Graphical comparison of results of displacement at free end and mid-span, stresses at integration point are presented in figures Fig (4.2) to (4.8). Tables (4.1) to (4.5) show the displacements at free end for different load increment and different numbers of elements. Table (4.6) and Fig (4.5) present the deflected (deformed) shape along center line. Figures (4.6) to (4.8) and Tables (4.7) to (4.9) show the stresses at integration point one as shown in Fig (3.4) and El (1) in Fig (4.2).

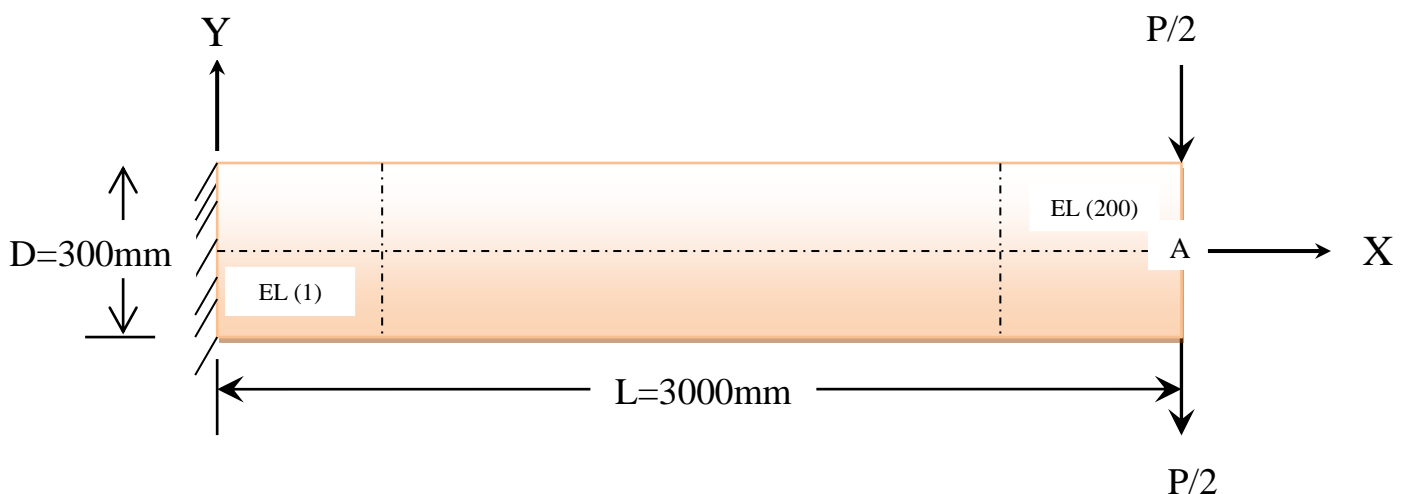


Fig (4-2) Cantilever plate beam with vertical load at free end

Table (4-1) Vertical displacement (10^{-1} mm) at free end and effect of mesh

Load(N)	Max load 3000N									
	20EL	40EL	60EL	80EL	100EL	120EL	140EL	160EL	180EL	200EL
Elements	20EL	40EL	60EL	80EL	100EL	120EL	140EL	160EL	180EL	200EL
Mesh	2*10	2*20	2*30	2*40	2*50	2*60	2*70	2*80	2*90	2*100
Aspect	2	1	0.667	0.5	0.40	0.334	0.285	0.25	0.222	0.2
V(mm)	6.77	8.526	8.957	9.120	9.197	9.239	9.265	9.282	9.294	9.36
Mesh	4*5	4*10	4*15	4*20	4*25	4*30	4*35	4*40	4*45	4*50
Aspect	8	4	2.667	2	1.6	1.333	1.143	1	0.888	0.8
V(mm)	3.191	6.859	8.112	8.669	8.95	9.118	9.219	9.287	9.334	9.367

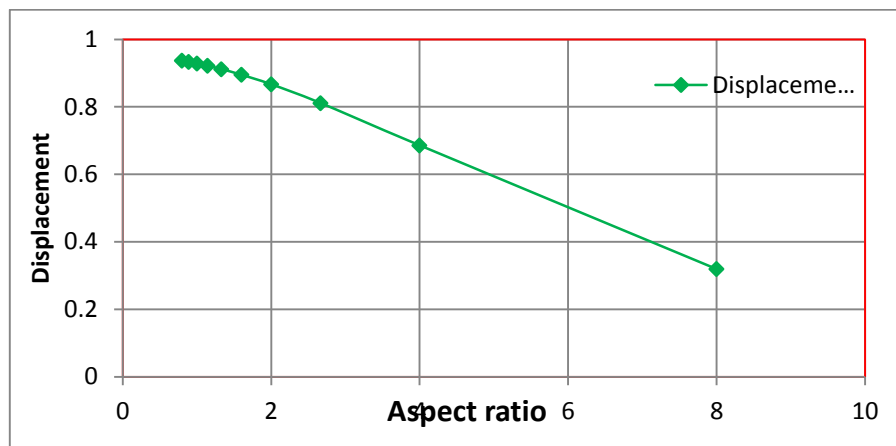


Fig (4-3) Effect of mesh and aspect ratio on accuracy of result

Table (4-2) Vertical displacement at free end in point A

Load(N)	Vertical displacement(mm)								
	60E	80E	100E	120E	140E	160E	180E	200E	Exact Sol
0	0	0	0	0	0	0	0	0	0
3000	0.8957	.9120	.9197	.9239	.9265	.9282	.9294	0.936	1
6000	1.791	1.824	1.839	1.848	1.853	1.856	1.859	1.860	2
9000	2.687	2.736	2.759	2.772	2.780	2.785	2.788	2.791	3
12000	3.583	3.648	3.679	3.696	3.706	3.713	3.718	3.721	4
15000	4.479	4.560	4.598	4.620	4.633	4.641	4.647	4.651	5
18000	5.374	5.472	5.518	5.544	5.559	5.569	5.576	5.581	6
21000	6.270	6.384	6.438	6.468	6.486	6.498	6.506	6.511	7
24000	7.166	7.296	7.357	7.392	7.412	7.426	7.435	7.442	8

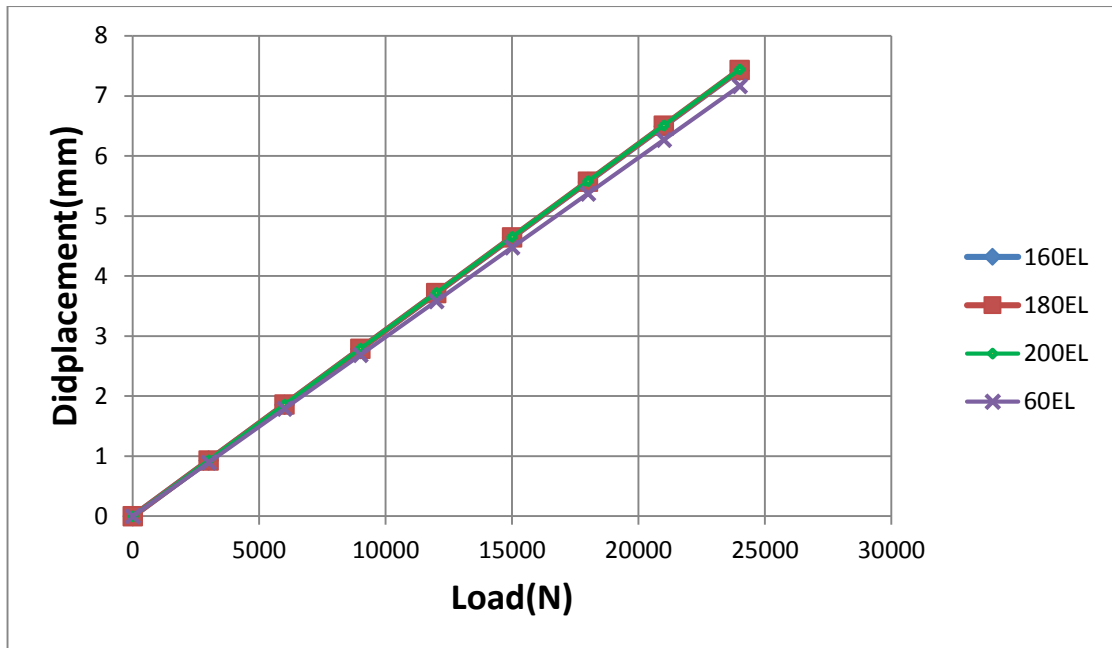


Fig (4-4) Vertical displacement at free end in point A

Table (4-3) Displacement at free end point A (200EI, 5INC)

Increment	Load 24000N
	V(mm)
0	0
1	1.488
2	2.977
3	4.465
4	5.953
5	7.442

Table (4-4) Displacement at free end point A (200EI, 10INC)

Increment	Load 24000N
	V(mm)
0	0
1	0.7442
2	1.488
3	2.233
4	2.977
5	3.721
6	4.465
7	5.209
8	5.953
9	6.698
10	7.442

Table (4-5) Displacement at free end point A (200 EI, 15INC)

Increment	Load 24000N	Increment	Load 24000N
	V(mm)		V(mm)
0	0	11	5.457
1	0.4961	12	5.953
2	0.9922	13	6.449
3	1.488	14	6.946
4	1.984	15	7.442
5	2.480		
6	2.976		
7	3.474		
8	3.969		
9	4.465		
10	4.961		

Table (4-6) Deflected shape along center line (100EI)

Node	Load 18000N	Load 21000N	Load 24000 N	Node	Load 18000N	Load 21000N	Load 24000 N
2	0	0	0	80	1.854	2.163	2.472
5	0.0009645	0.001125	0.001286	83	1.983	2.313	2.644
8	0.0117	0.01303	0.01489	86	2.115	2.467	2.820
11	0.0277	0.03242	0.03705	89	2.25	2.624	2.999
14	0.0506	0.05904	0.06748	92	2.387	2.785	3.183
17	0.07949	0.09274	0.106	95	2.528	2.949	3.37
20	0.1143	0.1334	0.1524	98	2.67	3.115	3.56
23	0.1549	0.1808	0.2066	101	2.815	3.285	3.754
26	0.2012	0.2348	0.2683	104	2.963	3.457	3.951
29	0.2531	0.2952	0.3374	107	3.112	3.631	4.15
32	0.3103	0.362	0.4137	110	3.264	3.808	4.352
35	0.3928	0.4349	0.4971	113	3.417	3.987	4.556
38	0.4405	0.5139	0.5873	116	3.572	4.168	4.763
41	0.5131	0.5986	0.6841	119	3.729	4.351	4.972
44	0.5907	0.6891	0.7875	122	3.887	4.535	5.183
47	0.6729	0.7851	0.8973	125	4.047	4.721	5.395
50	0.7598	0.8865	1.013	128	4.207	4.908	5.610
53	0.8512	0.9931	1.135	131	4.369	5.097	5.825
56	0.947	1.105	1.263	134	4.531	5.287	6.042
59	1.047	1.221	1.396	137	4.695	5.477	6.260
62	1.151	1.343	1.535	140	4.859	5.669	6.478
65	1.259	1.469	1.679	143	5.023	5.861	6.698
68	1.371	1.599	1.828	146	5.185	6.053	6.918
71	1.486	1.734	1.982	149	5.354	6.243	7.138
74	1.605	1.873	2.14	152	5.518	6.438	7.357
77	1.728	2.016	2.304				

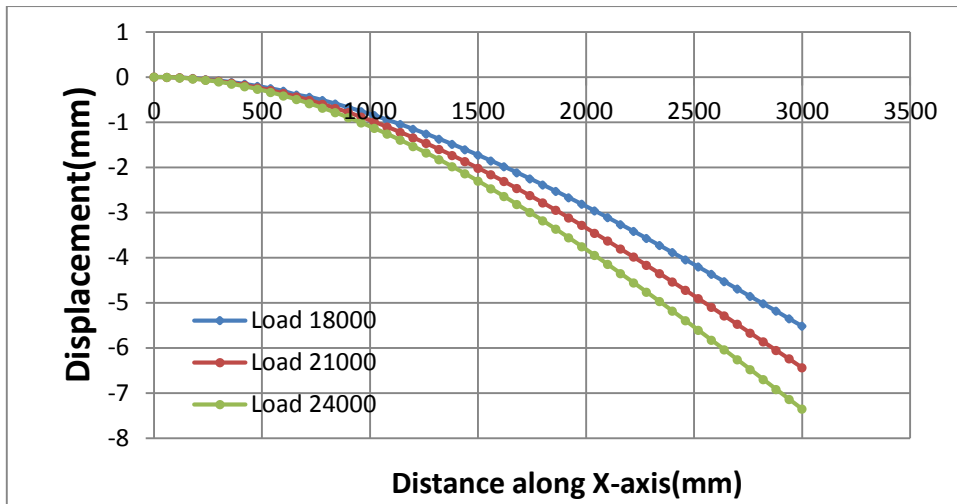


Fig (4-5) Deformed shape along center line

Table (4-7) Stress in x-direction at integration point (INT1, El (1))

Load(N)	Stresses (10^3N/mm^2)		
	160EL	180EL	200EL
0	0	0	0
3000	1.027	1.153	1.287
6000	2.142	2.413	2.684
9000	3.344	3.767	4.191
12000	4.633	5.22	5.807
15000	6.004	6.772	7.533
18000	7.477	8.422	9.369
21000	9.024	10.17	11.31
24000	10.66	12.02	13.37

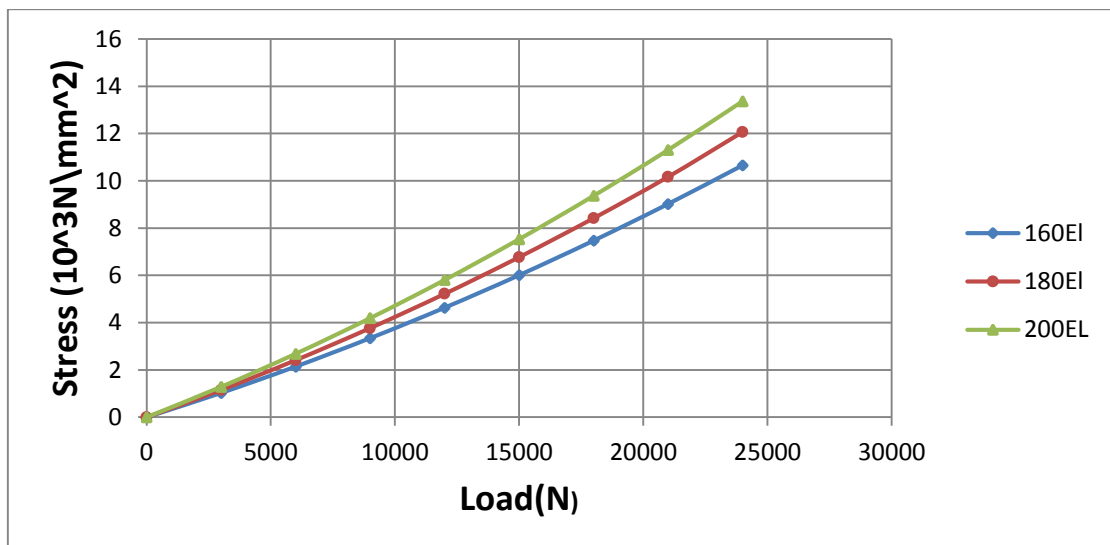


Fig (4-6) Stress in x-direction at integration point (INT 1, El 1)

Table (4-8) Stress in y-direction at integration point (INT 1, El (1))

Load(N)	Stresses (10^3N/mm^2)		
	160EL	180EL	200EL
0	0	0	0
3000	0.339	0.3819	0.4248
6000	0.7646	0.8617	0.9586
9000	1.277	1.439	1.601
12000	1.876	2.115	2.353
15000	2.561	2.88	3.214
18000	3.333	3.759	4.183
21000	4.192	4.728	5.262
24000	5.138	5.794	6.45

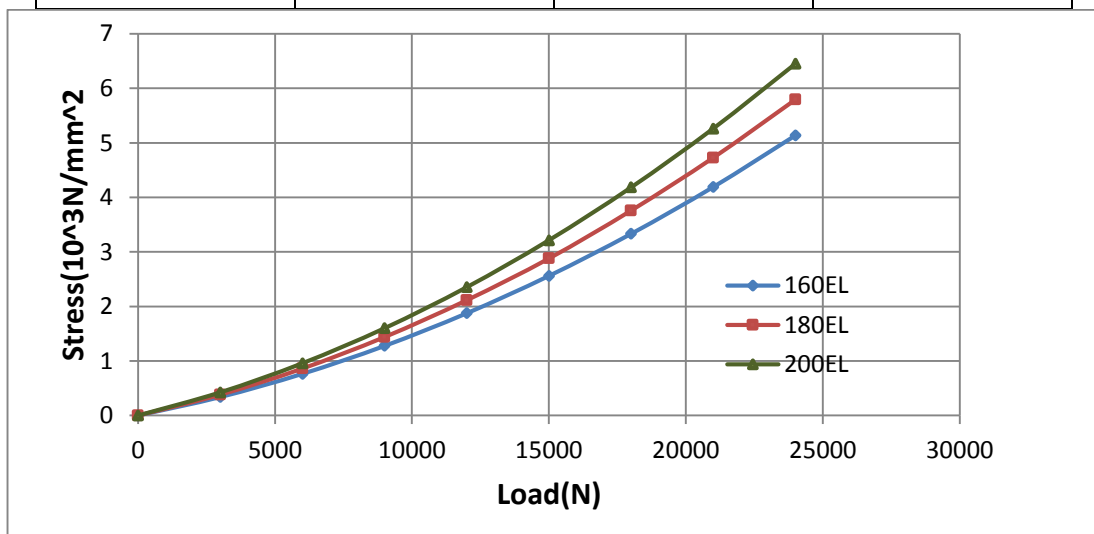


Fig (4-7) stress in y-direction at integration point (INT 1, El (1))

Table (4-9) Shear stress at integration point (INT 1, El (1))

Load(N)	Shear stresses (10^2N/mm^2)		
	160EL	180EL	200EL
0	0	0	0
3000	-1.918	-2.052	-2.186
6000	-3.836	-4.104	-4.372
9000	-5.754	-6.157	-6.558
12000	-7.673	-8.209	-8.744
15000	-9.591	-10.26	-10.93
18000	-11.51	-12.31	-13.12
21000	-13.43	-14.37	-15.3
24000	-15.35	-16.42	-17.49

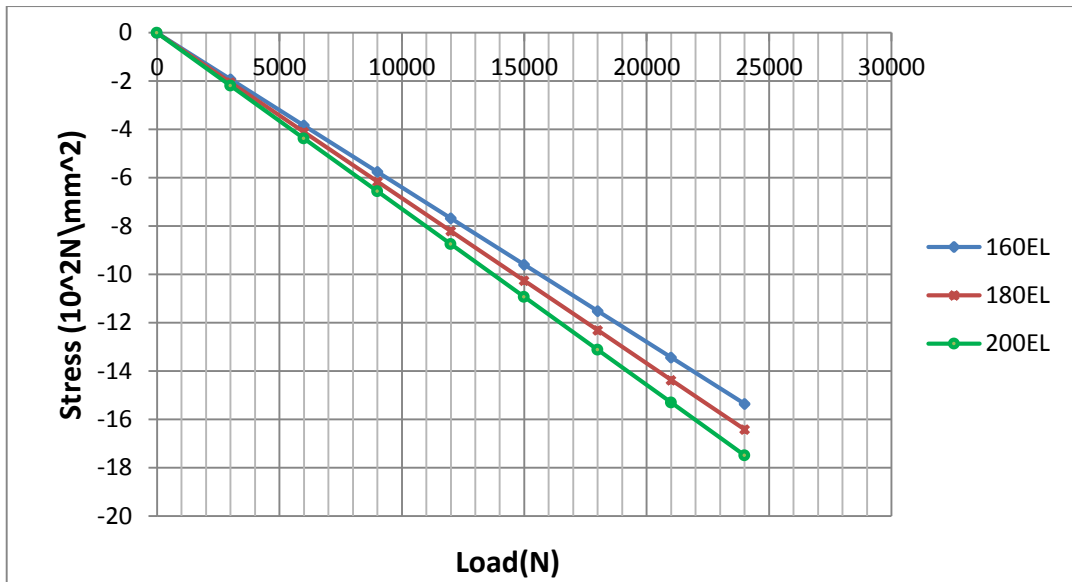


Fig (4-8) Shear stress at integration point (INT 1, El (1))

4.2.2.2 Cantilever plate beam under pure bending

A cantilever plate subjected to pure bending moment is considered, the cantilever is of dimensions $L=3000\text{mm}$, $D=300\text{mm}$ and thickness $h=60\text{mm}$ as shown in figure (4.9). The numerical values of material property parameter are: Young's modulus $E=210 \times 10^3 \text{N/mm}^2$, Poisson's ratio $\nu = 0.3$. The structure is modeled with different number of isoparametric elements. The mesh is of equal size of $150\text{mm} \times 150\text{mm}$, to check the accuracy of results of displacements and stresses they are compared for different numbers of elements, and with exact solutions. The results are presented in Figures (4.10) to (4.15) and tables (4.10) to (4.18). The vertical displacements with different numbers of elements are shown in tables (4.10) to (4.14) and figures (4.10) to (4.11). Tables (4.15) and Fig (4.12) show the deflected (deformed) shape along center line. The stresses at integration point are presented in tables (4.16) to (4-18) and Figures (4.13) to (4.15)

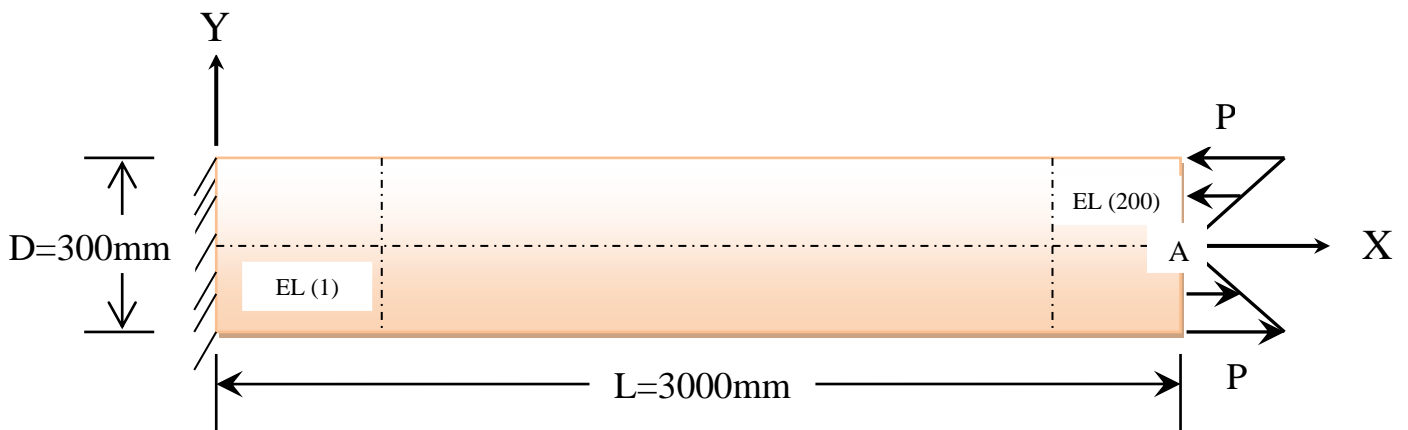


Fig (4.9) Cantilever plate under pure bending

Table (4-10) Vertical displacement ($\times 10^{-2}$) at free end with aspect ratio

Load(N)	Max load 3000N									
Elements	20EL	40EL	60EL	80EL	100EL	120EL	140EL	160EL	180EL	200E
Mesh	2*10	2*20	2*30	2*40	2*50	2*60	2*70	2*80	2*90	2*100
Aspect	2	1	0.667	0.5	0.40	0.334	0.285	0.25	0.222	0.2
V(mm)	5.051	6.357	6.678	6.798	6.855	6.887	6.906	6.918	6.927	6.93
Mesh	4*5	4*10	4*15	4*20	4*25	4*30	4*35	4*40	4*45	4*50
Aspect	8	4	2.667	2	1.6	1.333	1.143	1	0.888	0.8
V(mm)	-	5.292	6.052	6.464	6.675	6.796	6.871	6.920	6.955	6.979

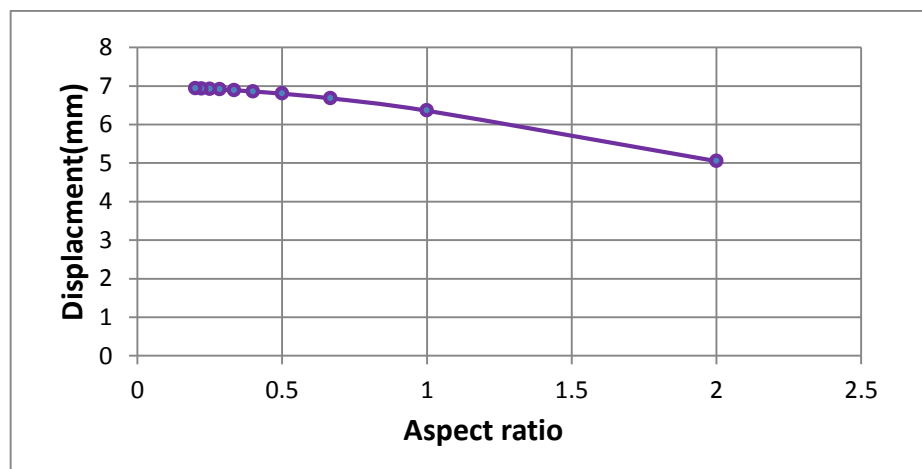


Fig (4-10) Effect of mesh and aspect ratio on accuracy of result

Table (4-11) Vertical displacement at free end point A

Load(N)	Vertical displacement(mm)								
	60E	80E	100E	120E	140E	160E	180E	200E	Exact
0	0	0	0	0	0	0	0	0	0
3000	.06678	.06798	.06855	.06887	.0691	.06918	.0693	.0693	0.071428
6000	0.1336	0.1360	0.1371	0.1377	0.138	0.1384	0.138	0.1387	0.142857
9000	0.203	0.2039	0.2057	0.2066	0.207	0.2076	0.207	0.208	0.214285
12000	0.2671	0.2719	0.2742	0.2755	0.276	0.2767	0.277	0.2773	0.285714
15000	0.3339	0.3399	0.3428	0.3443	0.345	0.3459	0.346	0.3467	0.357142
18000	0.4007	0.4079	0.4113	0.4132	0.414	0.4151	0.415	0.416	0.428571
21000	0.4674	0.4759	0.4799	0.4821	0.483	0.4843	0.484	0.4853	0.500000
24000	0.534	0.5438	0.5488	0.5514	0.552	0.5535	0.554	0.5547	0.571428

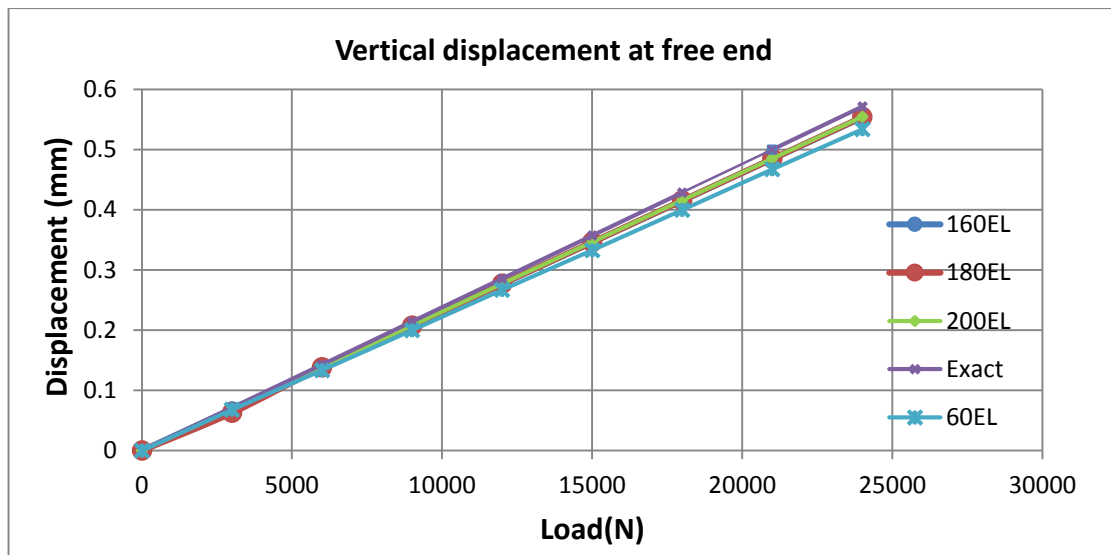


Fig (4-11) Vertical displacement at free end point A

Table (4-12) Displacement at free end point A (200 El, 4inc)

Increment	Load 24000N
	V(mm)
0	0
1	1.04
2	2.08
3	3.12
4	4.16

Table (4-13) Displacement at free end point A (200 EI, 8inc)

Increment	Load 18000N
	V(mm)
0	0
1	0.52
2	1.04
3	1.56
4	2.08
5	2.6
6	3.12
7	3.64
8	4.16

Table (4-14) Displacement at free end point A (200 EI, 12inc)

Increment	Load 18000N
	V(mm)
0	0
1	0.347
2	0.695
3	1.041
4	1.387
5	1.733
6	2.08
7	2.427
8	2.77
9	3.12
10	3.467
11	3.813
12	4.16

Table (4-15) Deflected shape along center line (60EI)

Node	Load 12000N	Load 15000N	Load 18000 N	Node	Load 12000N	Load 15000N	Load 18000 N
2	0	0	0	80	20.0	25.07	30.0
5	0.01772	0.02215	0.02658	83	21.63	27.04	32.44
8	0.1066	0.1333	0.1599	86	23.26	29.08	34.9
11	0.2536	0.317	0.3804	89	24.96	31.20	37.4
14	0.4602	0.5753	0.609	92	26.71	33.30	40.0
17	0.7264	0.908	1.09				
20	1.052	1.315	1.578				
23	1.437	1.796	2.156				
26	1.882	2.352	2.822				
29	2.386	2.982	3.578				
32	2.949	3.686	4.424				
35	3.572	4.465	5.358				

38	4.255	5.318	6.382
41	4.997	6.246	7.495
44	5.798	7.247	8.697
47	6.659	8.324	9.988
50	7.579	9.471	11.37
53	8.559	10.7	12.84
56	9.599	12.0	14.4
59	10.7	13.37	16.05
62	11.86	14.82	17.78
65	13.07	16.34	19.61
68	14.35	17.94	21.53
71	15.69	19.61	23.53
74	17.08	21.35	25.63
77	18.54	23.17	27.81

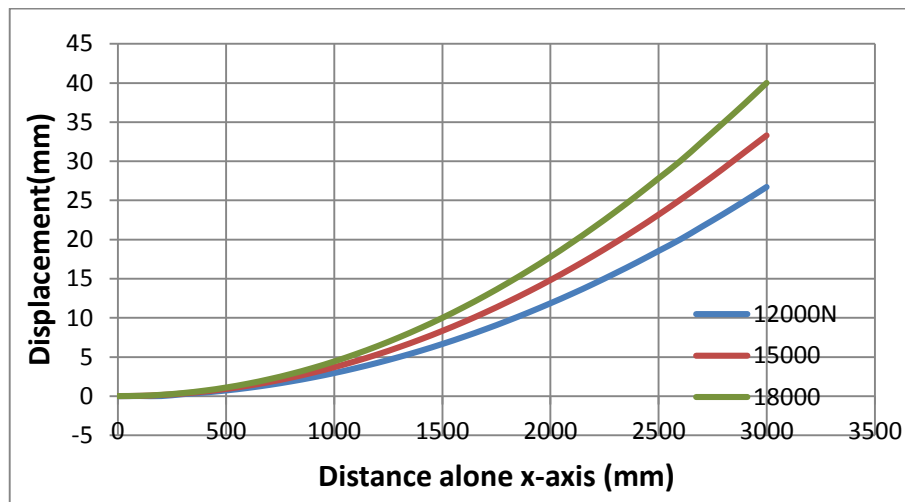


Fig (4-12) Deformed shape along center line

Table (4-16) Stress in x-direction at integration point (El 1, INT 1)

Load(N)	Stresses ($10^{-1}N/mm^2$)		
	160EL	180EL	200EL
0	0	0	0
3000	1.041	1.043	1.044
6000	2.081	2.085	2.088
9000	3.122	3.128	3.132
12000	4.163	4.17	4.176
15000	5.204	5.213	5.22
18000	6.245	6.256	6.264
21000	7.286	7.299	7.309
24000	8.327	8.341	8.353

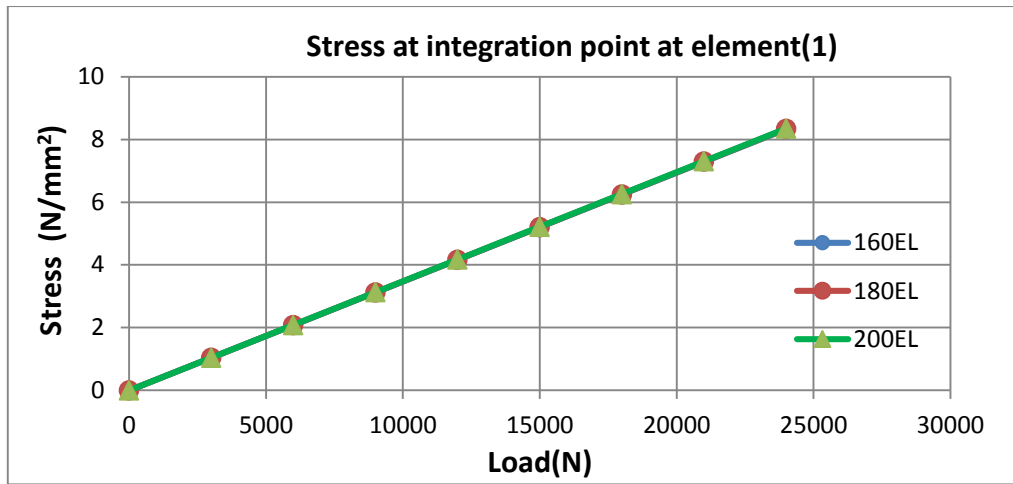


Fig (4-13) stress in x-direction at integration point (El 1, INT 1)

Table (4-17) Stress in y-direction at integration point (El 1, INT 1)

Load(N)	Stresses ($10^{-1}N/mm^2$)		
	160EL	180EL	200EL
0	0	0	0
3000	0.1909	0.1987	0.2057
6000	0.3819	0.3975	0.4114
9000	0.5728	0.5962	0.6171
12000	0.763	0.795	0.8228
15000	0.9548	0.9938	1.029
18000	1.146	1.193	1.234
21000	1.337	1.391	1.44
24000	1.528	1.59	1.646

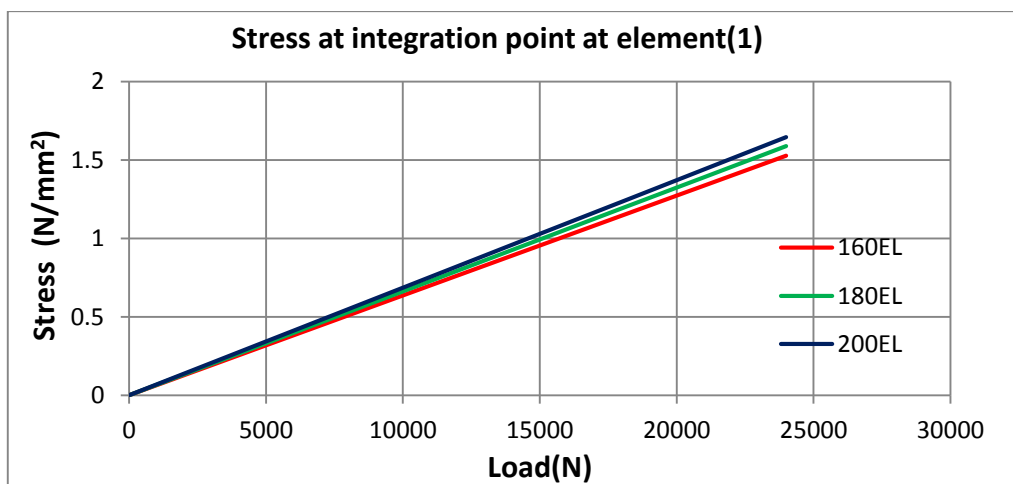


Fig (4-14) stress in y-direction at integration point (El 1, INT 1)

Table (4-18) Shear Stress at integration point (El 1, INT 1)

Load(N)	Shear stresses ($10^{-1}N/mm^2$)		
	160EL	180EL	200EL
0	0	0	0
3000	-0.1257	-1.549	-0.1792
6000	-0.2514	-0.3097	-0.3584
9000	-0.3771	-0.4646	-0.5376
12000	-0.5029	-0.6195	-0.7168
15000	-0.6286	-0.7743	-0.896
18000	-0.7543	-0.9292	-1.075
21000	-0.88	-1.084	-1.254
24000	-1.06	-1.23	-1.434

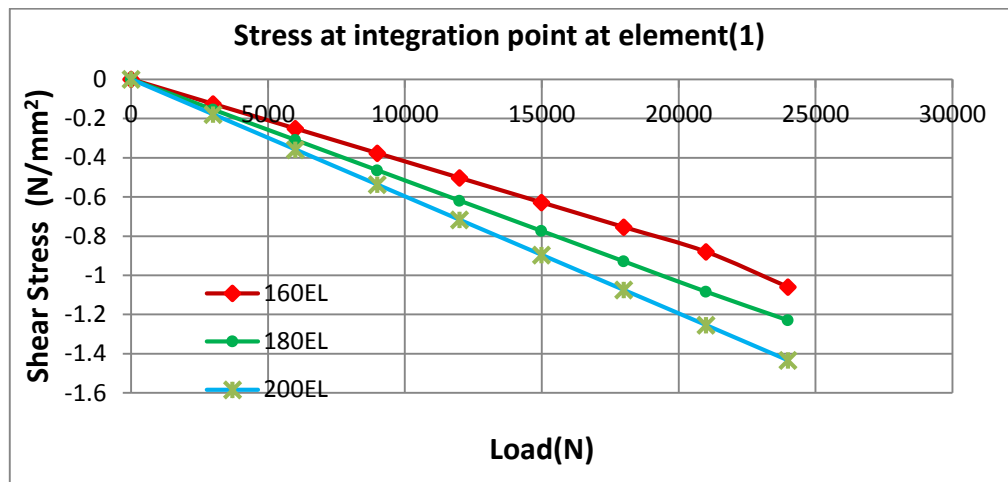


Fig (4-15) Shear stress at integration point (El 1, INT 1)

4.2.2.3- Simply Supported Plate Beam under Distributed Uniform Load

A beam with two-simple supported end is considered. The beam is of length $L=200mm$, height $D=10mm$, and thickness $1mm$, as shown in Fig (4.16). The numerical values for material property parameters are Young's modulus, $E=210GPa$, Poisson's ratio, $\nu=0.3$. The beam is modeled with a different numbers of mesh sizes.

The variation of the displacement and max deflection at the mid-span with different numbers of load increment are computed using Green formulation, and compared with the exact solution. Also the stresses at integration point

calculated for the different loading increment. Tables (4.20) and Fig (4.17) show the vertical displacements at mid-span, Table (4.12) and Fig (4.18) show the Deformation shape along center line. The stresses at integration point presented in Tables (4.22) to (4.23), Fig (4.19) to (4.20).

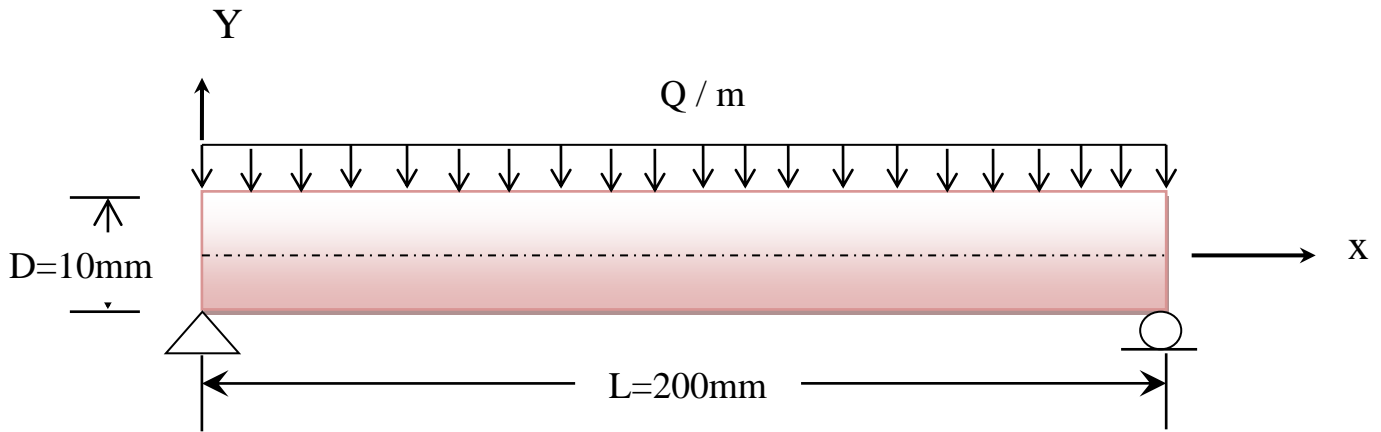


Fig (4-16) simple supported plate beam under distributed uniform load

Table (4-19) Vertical displacement at the mid span

Load(N)	Max load 1000N							
Elements	80EL	100EL	120EL	140EL	180EL	220EL	260EL	300EL
U(mm)	0	0	0	0	0	0	0	0
V(mm)	-1.713	-7.419	-7.744	-8.012	-8.316	-8.485	-8.591	-8.661

Table (4-20) Vertical displacement at mid span

Load(N)	Vertical displacement(mm)		
	220EL	260EL	300EL
0	0	0	0
1000	-4.243	-4.295	-4.331
2000	-8.485	-8.591	-8.661
3000	-12.73	-12.89	-12.99
4000	-16.97	-17.18	-17.32
5000	-21.21	-21.48	-21.65
6000	-25.46	-25.77	-25.98
7000	-29.7	-30.0	-30.31
8000	-33.94	-34.36	-34.64

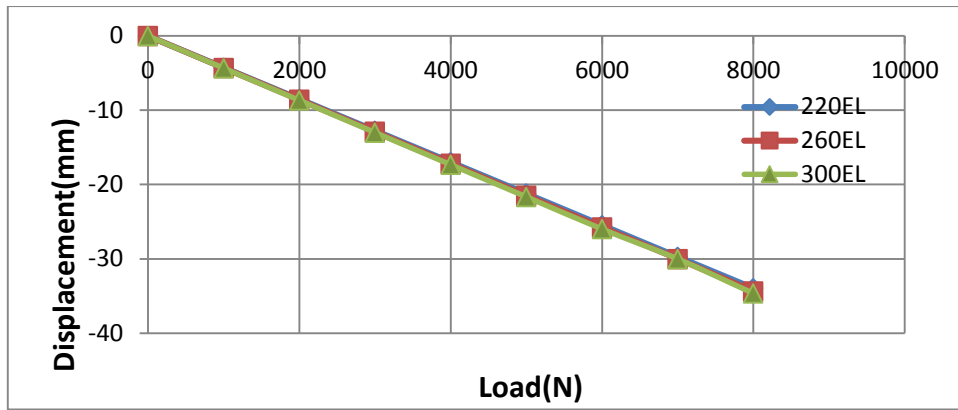


Fig (4-17) Vertical displacement at mid span

Table (4-21) Deflected shape along center line (220El)

Node	Load 4000N	Load 5000 N	Node	Load 4000N	Load 5000 N
3	0.05241	0.06551	143	-16.94	-21.18
8	-0.5564	-0.6955	148	-16.82	-21.03
13	-1.208	-1.51	153	-16.62	-20.78
18	-1.907	-2.383	158	-16.35	-20.43
23	-2.639	-3.299	163	-16.0	-20.0
28	-3.402	-4.252	168	-15.58	-19.48
33	-4.188	-5.236	173	-15.10	-18.88
38	-4.994	-6.243	178	-14.57	-18.21
43	-5.814	-7.268	183	-13.99	-17.48
48	-6.642	-8.303	188	-13.36	-16.69
53	-7.474	-9.342	193	-12.68	-15.86
58	-8.303	-10.38	198	-11.98	-14.97
63	-9.125	-11.41	203	-11.24	-14.05
68	-9.935	-12.42	208	-10.47	-13.09
73	-10.73	-13.41	213	-9.69	-12.11
78	-11.49	-14.37	218	-8.89	-11.11
83	-12.23	-15.29	223	-8.079	-10.10
88	-12.94	-16.18	228	-7.263	-9.079
93	-13.61	-17.01	233	-6.447	-8.05
98	-14.23	-17.79	238	-5.636	-7.046
103	-14.8	-18.50	243	-4.836	-6.044
108	-15.32	-19.15	248	-4.05	-5.062
113	-15.78	-19.72	253	-3.248	-4.105
118	-16.17	-20.21	258	-2.544	-3.180
1123	-16.49	-20.61	263	-1.834	-2.293
128	-16.73	-20.92	268	-1.159	-1.449
133	-16.9	-21.12	273	-0.5314	-0.6643
138	-16.97	-21.21	278	-0.0533	-0.0674

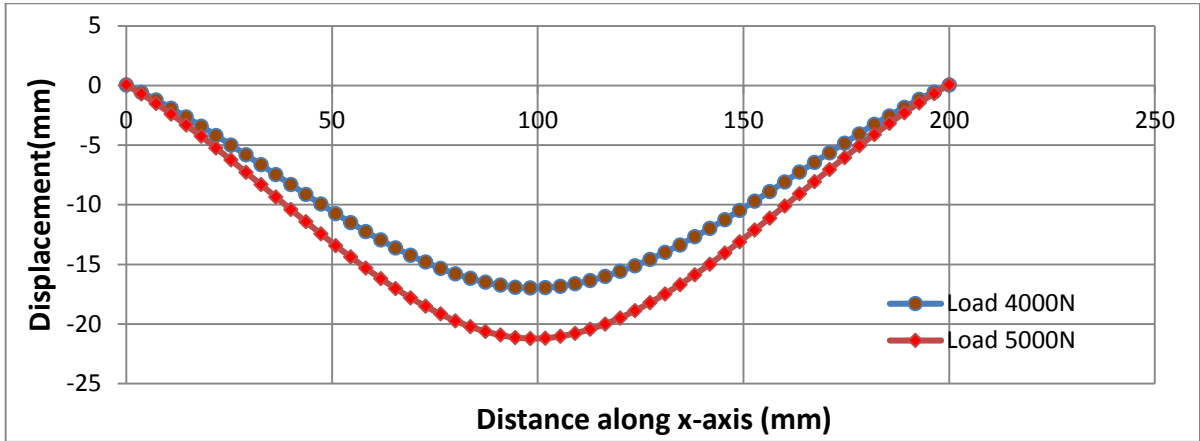


Fig (4-18) Deformed shape along center line

Table (4-22) Stress in x-direction at integration point at mid-span (INT 1)

Load(N)	Stresses(N/mm ²)	
	220EL	300EL
0	0	0
1000	0.0367	0.04779
2000	0.1818	0.2589
3000	0.4352	0.6332
4000	0.7968	1.17
5000	1.267	1.872
6000	1.845	2.736
7000	2.532	3.76
8000	3.327	4.954

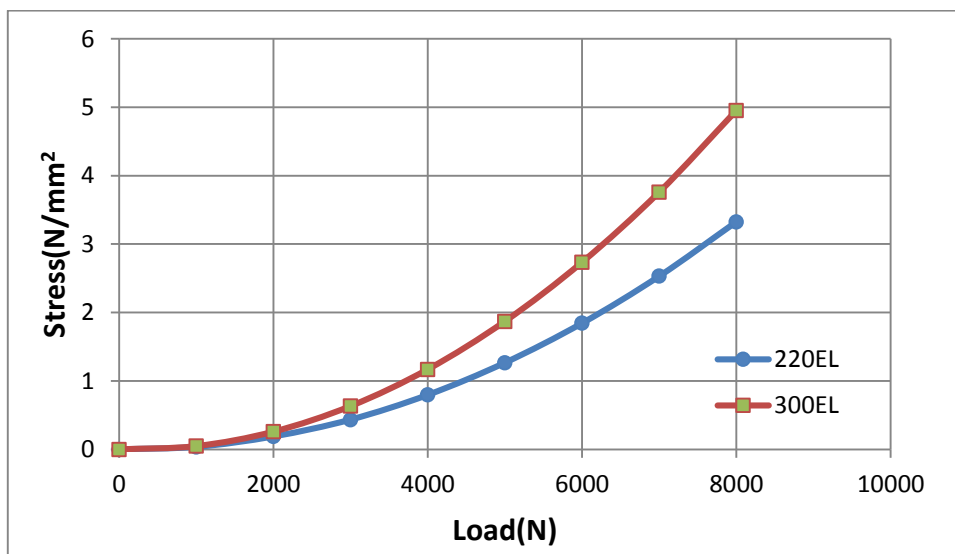


Fig (4-19) stress in x-direction at integration point at mid-span (INT 1)

Table (4-23) Stress in x-direction at integration point at mid-span (INT 1)

Load(N)	Stresses(N/mm ²)	
	260EL	300EL
0	0	0
1000	-0.218	-0.1103
2000	-0.6949	-0.5435
3000	-1.43	-1.30
4000	-2.425	-2.379
5000	-3.678	-3.78
6000	-5.189	-5.505
7000	-6.90	-7.553
8000	-8.989	-9.924

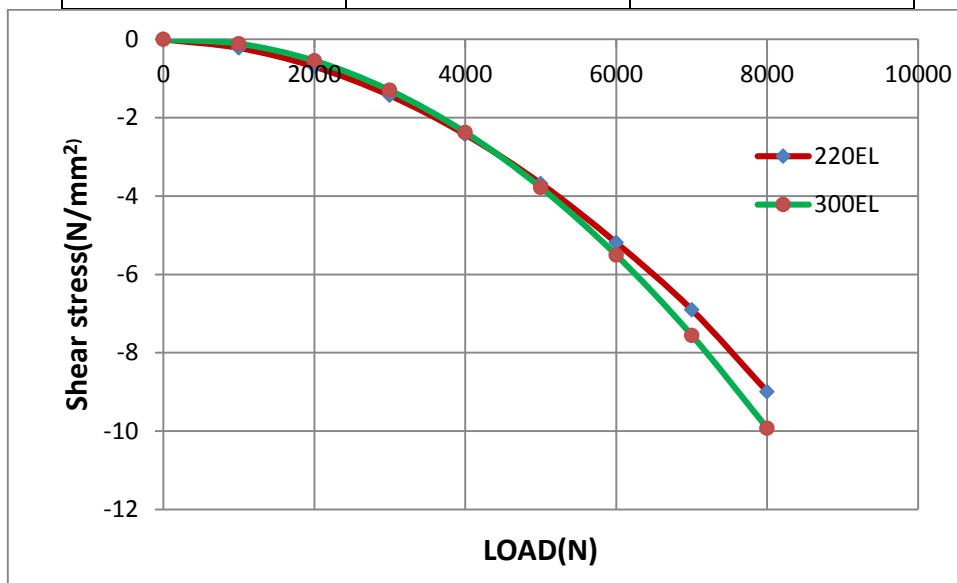


Fig (4-20) Shear stress in x-direction at integration point at mid-span (INT 1)

4.2.3 Nonlinear analysis:

4.2.3.1 Clamped plate beam under central Point load

A plate beam with two-fixed ends is considered. The plate beam is of length $L=200\text{mm}$, depth $D=10\text{mm}$ and thickness 1mm as shown in Fig (4.15). The numerical values of material property parameter are: Young's modulus $E=210 \times 10^3 \text{N/mm}^2$, Poisson's ratio $\nu = 0.3$. The structure is modeled with different number of elements. The mesh is of rectangular size of $20 \times 5\text{mm}$. The displacements, direct stresses and shear stresses obtained were compared for different numbers of elements and known results. The results are presented in Tables (4.24) and (4.25) and Fig (4.22) to (4.23). The vertical displacements at mid span are shown in Table (4.24) and Fig (4.22). Table (4.25) and Fig (4.23) show the deflected (deformed) shape along center line.

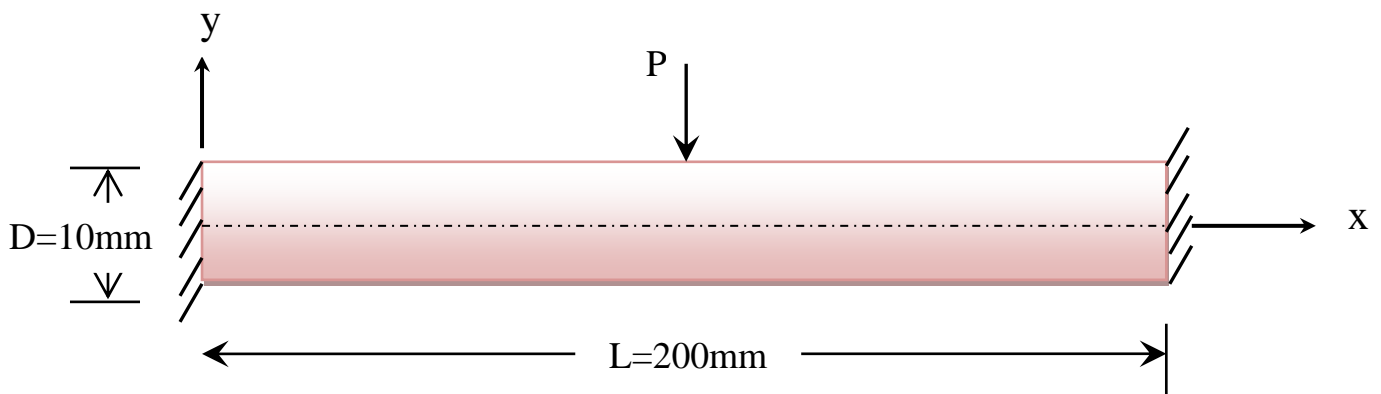


Fig (4-21) Clamped plate beam under concentrated load

Table (4-24) Displacement at mid-span

Load(N)	GREEN	Ref(3)
0	0	0
25	0.062	0.062
50	0.1067	0.126
100	0.231	0.253
175	0.50	0.449
287.5	0.8	0.751
456.25	1.26	1.122

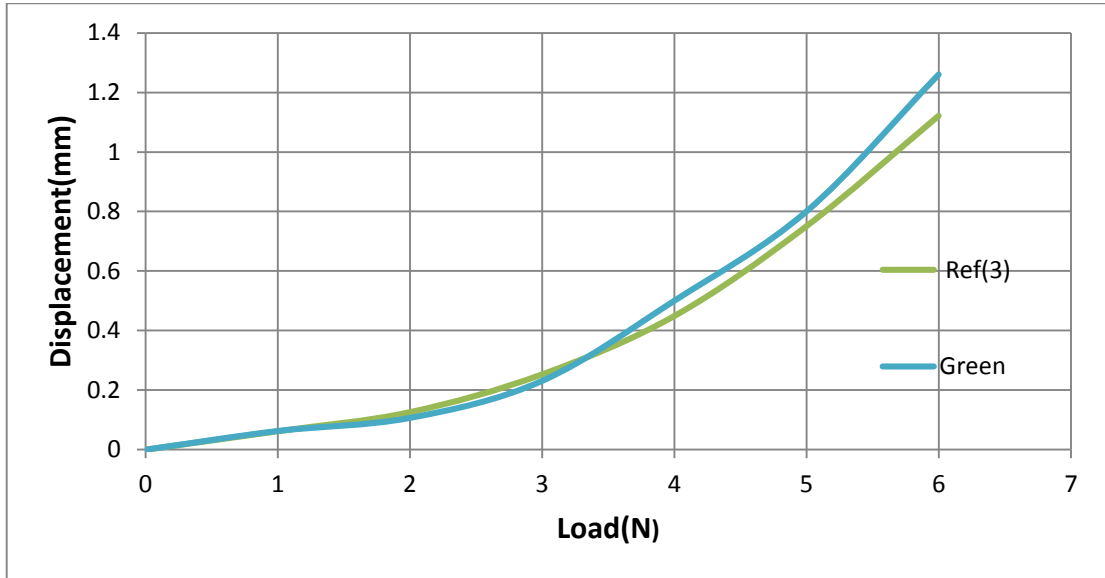


Fig (4-22) Vertical displacement at mid-span

Table (4-25) Deformed shape along center line (10^{-1} mm)

Node	Load 287.5N	Load 456.25N
2	0	0
5	-0.7487	-1.123
8	-2.317	-3.885
11	-4.208	-7.215
14	-6.154	-10.29
17	-8.0	-12.67
20	-9.575	-14.12
23	-10.42	-14.1
26	-9.515	-14.14
29	-5.054	-3.626
32	0	0

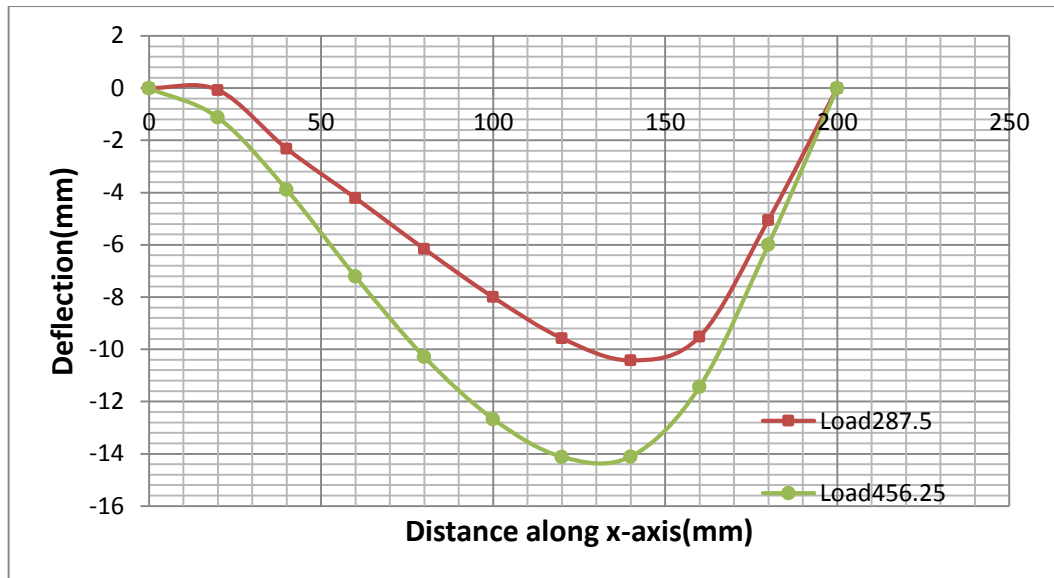


Fig (4-23) Deformed shape along center line

4.2.3.2 Cantilever plate beam under pure bending

A cantilever plate subjected to pure bending moment is adopted. The cantilever is of dimensions $L=3000\text{mm}$, $D=300\text{mm}$ and thickness $h=60\text{mm}$ as shown in Fig (4.24). The numerical values of material property parameter are: Young's modulus $E=210 \times 10^3 \text{N/mm}^2$, Poisson's ratio $\nu = 0.3$. The structure is modeled with different numbers of isoparametric elements. The mesh is of equal size of $150\text{mm} \times 150\text{mm}$, to check results the displacements and stresses compared for different numbers of elements, and the known result. The results are shown in Tables (4.26) and (4.27) and Fig (4.4.25) and (4.26). Table (4.26) and Fig (4.25) show the vertical displacement at free end. Table (4.27) and Fig (4.25) show the deflected (deformed) shape along center line.

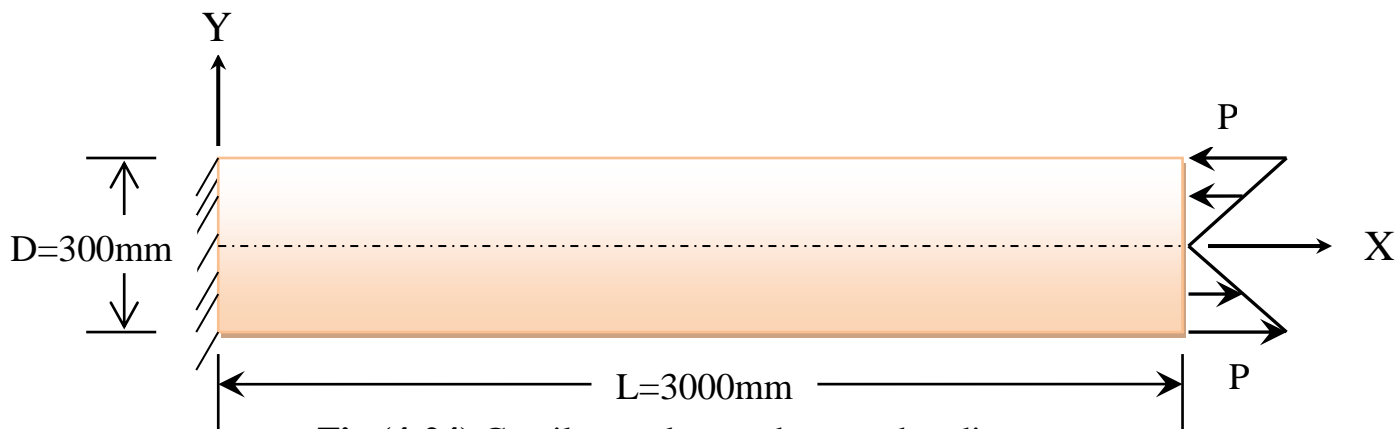


Fig (4-24) Cantilever plate under pure bending

Table (4-26) Vertical displacement at free end

Load(N)	GREEN	GREEN Ref(3)
0	0	0
3000	99.23	99.9727
6000	230.3	199.242
9000	344.2	297.087
12000	418	392.848
15000	493.5	485.959

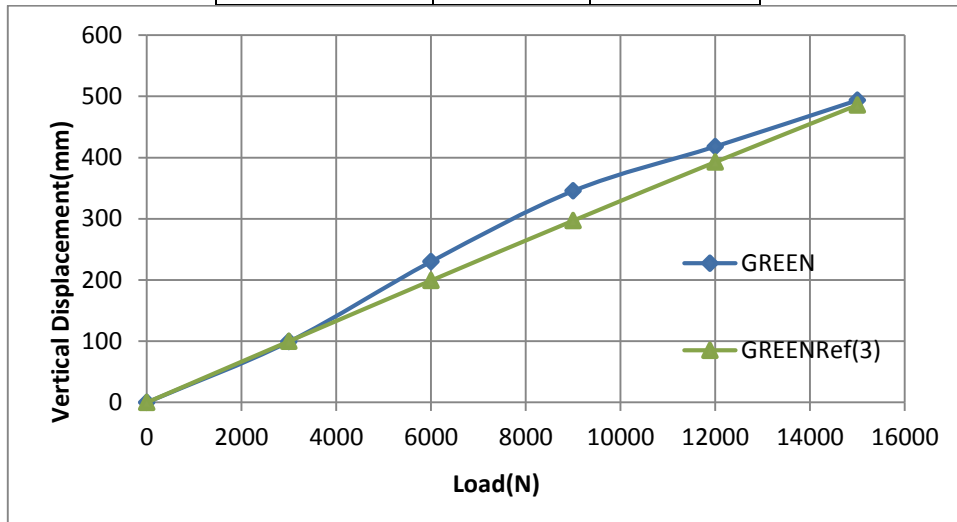


Fig (4-25) Vertical displacement at free end

Table (4-27) Deflected shape along center line

Node	GREEN3000N
35	2.53
38	6.563
41	11.01
44	15.79
47	20.81
50	26
53	31.25
56	36.49
59	41.62
62	46.55
65	51.22
58	55.53
71	59.43
74	62.84
77	65.72
80	68.03
83	69.71
86	70.7
89	71.14

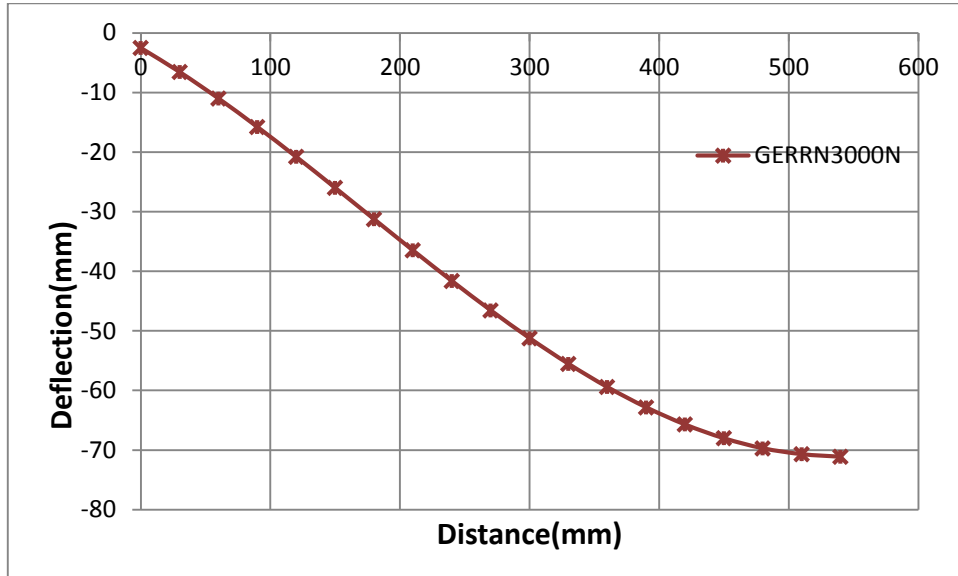


Fig (4-26) Deformed shape along center line

4.3 Discussion of Results

With reference to the results obtained from the application of the program, it can be stated that:

1- For the cantilever under tip load at free end the results are presented in table (4.1) to Table (4.9), and the Fig (4.1) to Fig (4.8), which demonstrate the efficiency of the linear analysis program.

Table (4.1) to Table (4.2) and Fig (4.3) show that the vertical displacements at free end for various applied loads and different numbers of elements are in agreement. The effect of aspect ratio and mesh refinement in the results are agreed with those presented by (Bhavikatti, 2005).

Fig (4.4) and Table (4.3) show that the displacement at point A at free end of structure, are in close agreement with that in exact solutions, Also, Fig (4.5) and Table (4.5) to Table (4.6) demonstrate that the deflected shape of the beam along center line and the displacement at free end. The stresses at the integration point show a good agreement for different numbers of elements and various applied loads.

Fig (4.3), Table (4.4), and Table (4.5) show the vertical displacement at free end for 5, 10, and 15 load increments and clearly demonstrate the accuracy of linear analysis results which are the same for all increments.

2- In the second example for linear analysis, the plate beam subjected to pure bending as shown in Fig (4.9) is analyzed. Fig (4.10) to Fig (15) and Table (4.10) to Table (4.18) show that the different values of displacements at the free end and direct stresses and shear stresses at integration points. Also, all values of the displacement and stresses are in very good agreement with exact solution. Fig (4-10) shows clearly the effect of the aspect ratio on the convergence of the results to the exact solution.

The numerical example is the simply supported plate beam under uniform load as in Fig (4-16). Fig (4-17) and Table (4-24) show the vertical displacement at the mid –span which is computed for different elements and different applied loads. The deformed shape along center line of beam is plotted in Fig (4-25), and the stresses at integration point are listed in Tables (4-25) and (4-26). All results are in good agreement with the exact solution.

3- For the nonlinear analysis, two numerical examples tested, cantilever plate beam subjected to pure bending, and clamped plat beam under concentrated load as shown in Fig (4.13) and Fig (4.14) respectively.

For the clamped plate beam, variation of displacement at mid-span with different load increment, and different iterations computed from the Green formulation as shown in Fig (4-22) and Table (4-24). The values of vertical displacements compared with those presented by (Akasha and Mohamed, 2012), these show good agreement. Also Fig (4-23) and Table (4-25) demonstrate the deformed shape of the beam and the effect of nonlinearity on the results.

For the case of the plate beam under pure bending, the displacement computed from Green formulation was compared with the results presented by (Akasha and Mohamed, 2012), as shown in Fig (4-25) and Table (4-26). These

show good agreement. Fig (4-26) and Table (4-28) represent the deformed shape for parts of the beam. The values demonstrate behavior of the structures that subjected to large deformation with different applied loads.

Chapter Five

Conclusions and recommendations

5.1 Summary of work

In this research the overall work can be summarized as follows:

- 1- The finite element computer program using standard MATLAB (2010b) language for analysis of static linear and nonlinear plane stresses/ strain structures have been developed.
- 2- The geometrically nonlinear formulation has been developed based on Total Lagrangian approach and Green strain using 2D plane stress/ strain 4-node isoparametric element.
- 3- The formulations for linear and geometrically nonlinear plane stress/ strain based on Green stress were implemented on computer using MATLAB as program, LINA2D for linear analysis and program NONLIA2D for nonlinear analysis.
- 4- The computer programs were tested using numerical examples and the results obtained were compared with published results.

5.2 Conclusions

Based on the results of numerical examples, it can be concluded that:

- 1- For the linear analysis the values of displacement, for any number of elements and various applied loads were in excellent agreement when compared with known results and exact solution. For cantilever under tip load, the maximum difference between the exact solution and program solution is about 6%, for mesh of 200 elements and with aspect ratio equal to 0.2. Also for the cantilever under pure bending and simple supported beam under udl, the maximum percentage differences between exact solution and linear program solution are 2.7% and 0.8% respectively.

2- For the nonlinear analysis the formulation based on Green strain give a good agreement when compared with known results, for various load increments and different iterations numbers. In case of clamped plate beam the difference between program results and those presented by (Akasha and Mohamed, 2012) is about 12%.

5.3 Recommendations

From the research results obtained, the following is recommended:

(1) Recommendation from study:-

- 1- Use of MATLAB programming language in developing finite element programs for its accuracy and ease of use.
- 2- Use of the program LINA2D in linear analysis of plane strain/stresses problems because it gives highly accurate results.

(2) Recommendation for future study:-

- 1- Modification of the program to calculate the average nodal stresses from the elements Gauss point results.
- 2- Developing the formulation to cover the gravity load and surface load
- 3- Developing the program to include higher order elements.
- 4- Extension of the nonlinear formulation to include engineering strain and logarithmic strain.
- 5- Developing the nonlinear formulations by using Updated Lagrangian formulation approach.
- 6- Extension of formulations to include nonlinear material, elastoplastic and hyperelastic materials.

REFERENCES

- [1] AbdElazeez, Ejlal, A.A., 2015, "Geometrically Nonlinear Finite Element Analysis of Cantilever Beam using MATLAB.
- [2] Adam, F. M, 2000, " Large Deformation finite element of Shell structures", MS.c Thesis, SUST, Sudan.
- [3] Akasha, N. M. and Mohamed, A. E, 2012, "Gometrically Nonlinear Analysis Using Plane Stress/strain Elements based on Alternative Strain Measures", Journal of Science and Technology, SUST, Khartoum, Sudan.
- [4] Akasha, N. M.,2009, " Development of Geometrically Nonlinear finite element Program Using Plane Stress/Strain Element Based on Engineering and True Stress Measures", Ph. D. Thesis, SUST, Khartoum, Sudan.
- [5] Akin, 2000, " Finite Element Analysis with Error Estimate", Houston. USA.
- [6] Bathe,K.J., Ramm, EK Ekhard. and Wilson, E. L, 1975, "Finite Element Formulations for Large Deformation Dynamic analysis", International Journal for Numerical Methods in Engineering, Vol.9, 353-386, California, U.S.A
- [7] Bathe. K, 1996, "Finite Element Procedures", Printic Hall Inc, USA.
- [8] Belytschison, Ted, Wing, K. L. and Brian. M, Khalil I. E, 2013, "Nonlinear Finite Elements Continua and Structures", Second Edition, John Wiley & Sons Ltd, Southern Gat, United Kingdom.
- [9] Bhavikatti, S.S, 2005, " Finite Element Analysis", New Age International, New Delhi, India.
- [10] Cook, D, 1995, "Finite Element Modeling For Stress Analysis", John Wiley & Sons Inc.USA.
- [11] Crisfield, M. A, 1991, "Nonlinear Finite Element Analysis of Solids and Structures ", John Wiley & Sons Ltd, Chichester, England.

- [12] Kattan P, 2008, "MATLAB Guide to Finite Elements an Interactive Approach", Springer, second edition, german.
- [13] Khennan, A., 2013, "Introduction to Finite Element Analysis Using MATLAB and ABAQUS ", Taylor &Francis Group, London, England.
- [14] Kim, N.H., 2014, "Introduction to Nonlinear Finite Element Analysis", spring science and Business Media New York, Gainesville, USA.
- [15] Mohamed, A. E. and Adam, F. M, 2003,"Finite Element Formulation of Large Deformation of Shells", Journal of Science andTechnology, SUST, Khartoum, Sudan.
- [16] Mohamed, A. E., Akasha, N. H, and Adam, F.A, 2013, "Evaluation of Engineering Stresses as the Correct Measure of Physical Stresses in Large Strain Geometrically Nonlinear Problems", International Journal of Engineering Inventions, Vol. 4,Issue8,PP 34-47.
- [18] Mohammed. M, 2009," Geometric Nonlinear Analysis of Isop- Quadrilatr Elements in 2D", Ph. D. Thesis, Springer, Felippa.
- [19] Rona, 1994," Finite Element Method for Geometrically Nonlinear Large Displacement Problems Thin, Elastic Plates and Shells", Ph,D Thesis, USA.
- [20] Young W. and Hyochoong B, 1997,"The finite Element Method Using MATLAB", CRC press, Washington, D.C. United States of America.
- [21] Zienkiewicz O. C. and Taylor R. L, 2000, "The Finite Element Method", Vol. 2, Butterworth-Heinemann, Spain.

Appendix A

The main function of program

```
clc
clear
clear all
%%%%%%%%%%%%%%%%%%%%%%%%%%%%%%%%%%%%%%%%%%%%%%%%%%%%%%%%%%%%%%%%%%%%%%%%
%
% -----the main program to solve the nonlinear program-----%
%%%%%%%%%%%%%%%%%%%%%%%%%%%%%%%%%%%%%%%%%%%%%%%%%%%%%%%%%%%%%%%%%%%%%%%%
%%%
%
global a0 %SIGMA
global NUMNP NE GXY LE NXE NYE dhx dhy X_0 Y_0
% inputs data
L=input('L=');
W=input('W=');
NXE=input('NXE=');
NYE=input('NYE=');
thick=input('thick=');
dhx=L/NXE;
dhy=W/NYE;
X_0=0;
Y_0=W/2;
% nodal coordinats and Element connectivity
[NUMNP, NDOF] = size(GXY);
NE = size(LE,1);
NEQ = NDOF*NUMNP;
% Material properties
PROP=[210000 0.3];
% Prescribed displacements [Node, DOF, Value]
pn1=((NXE+1)*(NYE+1)-2);
pn2=((NXE+1)*(NYE+1)-1);
pn3=(NXE+1)*(NYE+1);
SDISPT=[1 1 0;1 2 0;2 1 0;2 2 0;3 1 0;3 2 0];
% program parameters
TOL=1E-3;
% External forces [Node, DOF, Value]
EXF=input('EXF=');
xyD=input('xyD=');
%Fn1=((NXE+1)*(NYE+1)-2);
%Fn2=(NXE+1)*(NYE+1);
EXTFORCE=[Fn1 xyD EXF;Fn2 xyD -EXF];

% Check element connectivity
XYZON(GXY, LE, NOUT);
% Elastic modulus material properties
MID=1;
```

```

D=FORD (PROP,MID) ;
% initialize local and global matrixes and vectores
FG=zeros (NEQ,1) ;
GKT = zeros (NEQ,NEQ) ;
FORCE=zeros (NEQ,1) ;
EINF=zeros (8,1) ;
GINF=zeros (NEQ,1) ;
STRESS=zeros (3,1) ;
STRESS1=zeros (3,1) ;
DltS=zeros (3,1) ;
BL=zeros (3,8) ;
EK0=zeros (8,8) ;
EKL=zeros (8,8) ;
EKTsigma=zeros (8,8) ;
KET=zeros (8,8) ;
INC=input ('INC=') ;
FACTOR=1/INC ;
ITRA=input ('ITER=') ;
AnaType=input ('AnaType=') ;
a0=zeros (NEQ,1) ;
Dlta0=zeros (NEQ,1) ;

for Li=1:INC          % load
FG=zeros (NEQ,1) ;
% Assemble the global increment and external force vector
if size (EXTFORCE,1)>0
LOC = NDOF*(EXTFORCE (:,1)-1)+EXTFORCE (:,2) ;
Linc=FACTOR*EXTFORCE (:,3) ;
FG (LOC) = FG (LOC) + Linc ;
end
Dlta0=zeros (NEQ,1) ;
for ITER=1:ITRA      % Start convergence iteration(Newton-
Raphson)
if AnaType==1
FORCE=FG ;
else
FORCE=FG-GINF ;
end
%
% Integration points and weights
XG=[-0.577350269189630 -0.577350269189630;0.577350269189630 -
0.577350269189630;0.577350269189630 0.577350269189630;-
0.577350269189630 0.577350269189630] ;
WGT=[1 1 1 1] ;
%
GKT = zeros (NEQ,NEQ) ;
%LOOP OVER ELEMENTS, MAIN LOOP TO COMPUTE GKT
for IE=1:NE
% Element Nodal coordinates
ELXY=GXY (LE (IE,:), :) ;
% from Local to global
EKT=zeros (8,8) ;
%IDOF=zeros (1,8) ;

```

```

for I=1:4
II=(I-1)*NDOF+1;
IDOF (II:II+1)=(LE (IE, I) -1) *NDOF+1: (LE (IE, I) -1) *NDOF+2;
end
DSP=a0 (IDOF); % displacement vector
DSPD=Dlta0 (IDOF); % displacement increment vector
%LOOP OVER INTEGRATION POINTS
for LX=1:4
E1=XG (LX, :);
% Determinant and shape function derivatives
[DSF, SHPD, DET] = SHAPEL (E1, ELXY);
FAC=thick*DET*WGT (LX);
%
Bo=[SHPD (1, 1) 0 SHPD (1, 2) 0 SHPD (1, 3) 0
SHPD (1, 4) 0 ;
0 SHPD (2, 1) 0 SHPD (2, 2) 0
SHPD (2, 3) 0 SHPD (2, 4);
SHPD (2, 1) SHPD (1, 1) SHPD (2, 2) SHPD (1, 2) SHPD (2, 3)
SHPD (1, 3) SHPD (2, 4) SHPD (1, 4)];
%
G=[SHPD (1, 1) 0 SHPD (1, 2) 0 SHPD (1, 3) 0
SHPD (1, 4) 0 ;
0 SHPD (1, 1) 0 SHPD (1, 2) 0
SHPD (1, 3) 0 SHPD (1, 4);
SHPD (2, 1) 0 SHPD (2, 2) 0 SHPD (2, 3) 0
SHPD (2, 4) 0 ;
0 SHPD (2, 1) 0 SHPD (2, 2) 0
SHPD (2, 3) 0 SHPD (2, 4)];
% to forming thata
thata=G*DSP; % forming thata
dthata =G*DSPD; % forming Dlta thata
% to formin A thata
A=[thata (1) thata (2) 0 0; 0 0 thata (3) thata (4); thata (3)
thata (4) thata (1) thata (2)];
dA=[dthata (1) dthata (2) 0 0; 0 0 dthata (3) dthata (4); dthata (3)
dthata (4) dthata (1) dthata (2)];
% the strain displacement matrix B
BL=A*G;
BLd=dA*G;
B=Bo+BL;
%
% the strain increment
DltE=(Bo+BL+0.5*BLd)*DSPD;
% Stress incremental
DltS=D*DltE;
% Total Stresses
STRESS=STRESS+DltS;
% stress stiffness matrix
M=[STRESS (1) 0 STRESS (3) 0; 0 STRESS (1) 0 STRESS (3); STRESS (3) 0
STRESS (2) 0; 0 STRESS (3) 0 STRESS (2)];
% Tangent stiffness Matrix
EK0=FAC*Bo' *D*Bo;

```



```

EKL=FAC*Bo'*D*BL+BL'*D*Bo+BL'*D*BL;
EKTSigma=FAC*G'*M*G; % Element tangent
stiffness matrix
if AnaType==1
EKT=EKT+EK0;
else
EKT=EKT+EK0+EKL+EKTSigma;
end
end
GKT(IDOF, IDOF)=GKT(IDOF, IDOF)+EKT; % Global tangent
stiffness matrix
end
%
% Prescribed displacement BC
NDISP=size(SDISPT,1);
if NDISP~=0
FIXEDDOF=NDOF*(SDISPT(:,1)-1)+SDISPT(:,2);
GKT(FIXEDDOF,:)=zeros(NDISP,NEQ);
GKT(:,FIXEDDOF)=zeros(NEQ,NDISP);
GKT(FIXEDDOF,FIXEDDOF)=eye(NDISP);
FORCE(FIXEDDOF)=0;
end
% Check convergence
if (ITER>=0)
Conve=norm(FORCE,inf);
OUTPUT_1(ITER, Conve)
if ITER<ITRA && Conve<TOL
break;
end
end
% Check max iteration
if(ITER>ITRA), error('Iteration limit exceeds');
end

% Solve the system equation(the incremental displacement)
Dlta0= GKT\FORCE;
a0=a0+Dlta0;
%
Dlta01=Dlta0;
a01=a0;
GINF=zeros(NEQ,1);
INT=0;
% assemble Global atiffness matrix GINF
for IE=1:NE
% Element Nodal coordinates and incremental displacements
ELXY=GXY(LE(IE,:),:);
% Local to global
EINF=zeros(8,1);
IDOF=zeros(1,8);
for I=1:4
II=(I-1)*NDOF+1;
IDOF(II:II+1)=(LE(IE,I)-1)*NDOF+1:(LE(IE,I)-1)*NDOF+2;
end

```

```

DSP1=a01(IDOF);           % displacement vector
DSPD1=Dlta01(IDOF);      % displacement increment vector
%LOOP OVER INTEGRATION POINTS
for LX=1:4
E1=XG(LX,:);             % this values using to calculate cmponent
of jacobian
% Determinant and shape function derivatives
[DSF,SHPD,DET] = SHAPEL(E1, ELXY);
FAC=thick*DET*WGT(LX);
INT=INT+1;
Bo1=[SHPD(1,1) 0          SHPD(1,2) 0          SHPD(1,3) 0
SHPD(1,4) 0          ;
0          SHPD(2,1) 0          SHPD(2,2) 0
SHPD(2,3) 0          SHPD(2,4);
SHPD(2,1) SHPD(1,1) SHPD(2,2) SHPD(1,2) SHPD(2,3)
SHPD(1,3) SHPD(2,4) SHPD(1,4)];

G01=[SHPD(1,1) 0          SHPD(1,2) 0          SHPD(1,3) 0
SHPD(1,4) 0          ;
0          SHPD(1,1) 0          SHPD(1,2) 0
SHPD(1,3) 0          SHPD(1,4);
SHPD(2,1) 0          SHPD(2,2) 0          SHPD(2,3) 0
SHPD(2,4) 0          ;
0          SHPD(2,1) 0          SHPD(2,2) 0
SHPD(2,3) 0          SHPD(2,4)];

% to forming thata
thata1=G01*DSP1;        % forming thata
dthata1 =G01*DSPD1;    % forming Dlta thata

% to formin A thata
A1=[thata1(1) thata1(2) 0 0;0 0 thata1(3) thata1(4);thata1(3)
thata1(4) thata1(1) thata1(2)];
dA1=[dthata1(1) dthata1(2) 0 0;0 0 dthata1(3)
dthata1(4);dthata1(3) dthata1(4) dthata1(1) dthata1(2)];
%
% the strain displacement matrix B
BL1=A1*G01;
BLd1=dA1*G01;
B1=Bo+BL1;
%
% the strain increment
DltE1=(Bo+BL1+BLd1)*DSPD1;
%
% Stress incremental
DltS1=D*DltE1;
% Total Stresses
STRESS1=STRESS1+DltS1;
SIGMA(:,INT)=STRESS1;
% Residual internal forces
EINF=EINF+FAC*B1'*STRESS1;
end
end

```

```
GINF(IDOF) = GINF(IDOF) + EINF;      % Global internal forces
end
% print results
PROUT_1(NOUT, NUMNP, NDOF, NE);
end
```

Appendix B

Example of input data and print out of results

Input Data:

L=3000

W=300

NXE=5

NYE=2

thick=60

EXF=1500

xyD=1

INC=1

ITER=1

AnaType=1

Output results:

Iteration Residual

Nodal Displacements

Node	U	V
1	0.000e+000	0.000e+000
2	0.000e+000	0.000e+000
3	0.000e+000	0.000e+000
4	5.515e-004	1.116e-003
5	8.485e-018	1.090e-003
6	-5.515e-004	1.116e-003
7	1.110e-003	4.437e-003
8	1.498e-017	4.417e-003
9	-1.110e-003	4.437e-003

10	1.667e-003	9.993e-003
11	2.639e-017	9.971e-003
12	-1.667e-003	9.993e-003
13	2.225e-003	1.778e-002
14	3.739e-017	1.776e-002
15	-2.225e-003	1.778e-002
16	2.782e-003	2.779e-002
17	2.850e-017	2.777e-002
18	-2.782e-003	2.779e-002

Element Stress

	S1	S2	S12
Element	1		
	4.227e-002	4.912e-003	8.471e-002
	8.454e-002	9.828e-003	1.694e-001
	1.268e-001	1.474e-002	2.541e-001
	1.691e-001	1.966e-002	3.388e-001
Element	2		
	4.339e-003	-2.199e-002	4.256e-001
	-1.604e-001	-6.364e-002	5.123e-001
	-3.251e-001	-1.053e-001	5.991e-001
	-4.899e-001	-1.469e-001	6.858e-001
Element	3		
	-4.559e-001	-1.715e-001	7.729e-001
	-4.219e-001	-1.961e-001	8.601e-001
	-3.879e-001	-2.206e-001	9.472e-001
	-3.539e-001	-2.452e-001	1.034e+000
Element	4		

-5.120e-001	-2.578e-001	1.121e+000
-6.700e-001	-2.704e-001	1.208e+000
-8.280e-001	-2.831e-001	1.294e+000
-9.861e-001	-2.957e-001	1.381e+000
Element	5	
-9.499e-001	-3.127e-001	1.467e+000
-9.138e-001	-3.296e-001	1.554e+000
-8.777e-001	-3.466e-001	1.640e+000
-8.415e-001	-3.636e-001	1.727e+000
Element	6	
-1.001e+000	-3.836e-001	1.813e+000
-1.161e+000	-4.036e-001	1.900e+000
-1.321e+000	-4.237e-001	1.987e+000
-1.480e+000	-4.437e-001	2.073e+000
Element	7	
-1.445e+000	-4.626e-001	2.160e+000
-1.409e+000	-4.814e-001	2.247e+000
-1.373e+000	-5.003e-001	2.333e+000
-1.338e+000	-5.191e-001	2.420e+000
Element	8	
-1.497e+000	-5.372e-001	2.507e+000
-1.656e+000	-5.553e-001	2.593e+000
-1.815e+000	-5.733e-001	2.680e+000
-1.975e+000	-5.914e-001	2.767e+000
Element	9	
-1.939e+000	-6.097e-001	2.853e+000
-1.903e+000	-6.280e-001	2.940e+000

-1.867e+000	-6.463e-001	3.026e+000
-1.831e+000	-6.646e-001	3.113e+000
Element	10	
-1.991e+000	-6.831e-001	3.200e+000
-2.150e+000	-7.016e-001	3.286e+000
-2.309e+000	-7.201e-001	3.373e+000
-2.468e+000	-7.386e-001	3.460e+000